

Higher spins on AdS_3 from the worldsheet

Kevin Ferreira, Matthias R. Gaberdiel and Juan I. Jottar

Institut für Theoretische Physik, ETH Zurich,

CH-8093 Zürich, Switzerland

E-mail: kevinp@phys.ethz.ch, gaberdiel@itp.phys.ethz.ch,
jijottar@phys.ethz.ch

ABSTRACT: It was recently shown that the CFT dual of string theory on $\text{AdS}_3 \times \text{S}^3 \times \text{T}^4$, the symmetric orbifold of T^4 , contains a closed higher spin subsector. Via holography, this makes precise the sense in which tensionless string theory on this background contains a Vasiliev higher spin theory. In this paper we study this phenomenon directly from the worldsheet. Using the WZW description of the background with pure NS-NS flux, we identify the states that make up the leading Regge trajectory and show that they fit into the even spin $\mathcal{N} = 4$ Vasiliev higher spin theory. We also show that these higher spin states do not become massless, except for the somewhat singular case of level $k = 1$ where the theory contains a stringy tower of massless higher spin fields coming from the long string sector.

Contents

1	Introduction	1
2	Worldsheet string theory on AdS_3	4
2.1	The AdS_3 WZW model	5
2.1.1	The NS sector	6
2.1.2	The R sector	7
2.2	The compact directions	8
2.3	GSO projection	9
2.4	Physical state conditions	10
3	No massless higher spin states from short strings	12
4	Regge trajectories and their $\mathcal{N} = 4$ structure	14
4.1	General discrete spectrum	14
4.2	Leading Regge trajectory	17
4.3	Subleading $\mathcal{N} = 4$ trajectory	20
4.4	$\text{AdS}_3 \times \text{S}^3 \times \text{K3}$	21
5	Spectrally flowed sectors and long strings	22
5.1	Spectrally flowed representations — the continuous case	23
5.1.1	Massless higher spin fields for $k = 1$	24
5.2	Spectrally flowed representations — the discrete case	25
5.3	Comparison of the different sectors	27
6	Conclusions	28
A	Supersymmetric current algebras: conventions and useful formulae	29
B	Low momenta subtleties	32
C	The structure of small $\mathcal{N} = 4$ multiplets	33

1 Introduction

In the tensionless limit string theory is expected to exhibit a large underlying symmetry that is believed to lie at the heart of many special properties of stringy physics [1–3]. In flat space, the tensionless limit is somewhat subtle since there is no natural length scale relative to which the (dimensionful) string tension may be taken to zero. The situation is

much better in the context of string theory on an AdS background, since the cosmological constant of the AdS space defines a natural length scale. This is also reflected by the fact that higher spin theories – they are believed to capture the symmetries of the leading Regge trajectory at the tensionless point [4, 5] — appear naturally in AdS backgrounds [6].

In the context of string theory on AdS₃ concrete evidence for this picture was recently obtained in [7]. More specifically, it was shown that the CFT dual of string theory on AdS₃ × S³ × T⁴, the symmetric orbifold of T⁴, see [8] for a review, contains the CFT dual of the supersymmetric higher spin theories constructed in [9].¹ While this indirect evidence is very convincing, it would be very interesting to have more direct access to the higher spin sub-symmetry in string theory. This symmetry is only expected to emerge in the tensionless limit of string theory, in which the string is very floppy and usual supergravity methods are not reliable. Thus we should attempt to address this question using a worldsheet approach.

Worldsheet descriptions of string theory on AdS backgrounds are notoriously hard, but in the context of string theory on AdS₃, the background with pure NS-NS flux admits a relatively straightforward worldsheet description in terms of a WZW model based on the Lie algebra $\mathfrak{sl}(2, \mathbb{R})$ [16–18]. In this paper we shall use this approach to look for signs of a higher spin symmetry among these worldsheet theories. More concretely, we shall combine the WZW model corresponding to $\mathfrak{sl}(2, \mathbb{R})$ with an $\mathfrak{su}(2)$ WZW model, describing strings propagating on S³, as well as four free fermions and bosons corresponding to T⁴. The complete critical worldsheet theory then describes strings on AdS₃ × S³ × T⁴.

The worldsheet description of these WZW models contains one free parameter, the level k of the $\mathcal{N} = 1$ superconformal WZW models associated to $\mathfrak{sl}(2, \mathbb{R})$ and $\mathfrak{su}(2)$, respectively — these two levels have to be the same in order for the full theory to be critical. Geometrically, these levels correspond to the size of the AdS₃ space (and the radius of S³) in string units. The tensionless limit should therefore correspond to the limit where k is taken to be small.

In this paper we analyse systematically the string spectrum of the worldsheet theory for k small.² As we shall show, the only massless spin fields that emerge in this limit are those associated to the supergravity multiplet, while all the higher spin fields remain massive, except in the extremal case where the level is taken to be $k = 1$ — this is strictly speaking an unphysical value for the level since then the bosonic $\mathfrak{su}(2)$ model has negative level; however, as argued in [23], some aspects of the theory may still make sense. (We should also mention that in the context of the WZW model based on AdS₃ × S³ × S³ × S¹ [24, 25] the theory with $k = 1$ is not singular since it is compatible with the levels of the two superconformal $\mathfrak{su}(2)$ models being $k^+ = k^- = 2$, leading to vanishing bosonic levels

¹Superconformal higher spin theories were first constructed in [10, 11]. The duality is the natural supersymmetric analogue of the original bosonic proposal of [12], see [13] for a review; various properties of the $\mathcal{N} = 4$ duality were further analysed in [14, 15].

²See e.g. [19–22] and references therein for other worldsheet approaches to this problem which do not focus on the spectrum itself, but rather on the symmetry structures that are presumed to emerge in the tensionless limit of string theory.

for the two $\mathfrak{su}(2)$ algebras.)³ For $k = 1$, the bosonic $\mathfrak{sl}(2, \mathbb{R})$ algebra has level $k_{\text{bos}} = 3$, and as in [26], an infinite tower of massless higher spin fields arises from the long string subsector (the spectrally flowed continuous representations). These higher spin fields are part of a continuum and realise quite explicitly some of the speculations of [23].

For more generic values of the level, we also explain the sense in which a ‘leading Regge trajectory’ emerges, and we give an explicit description of these states. In particular, we show that the relevant states form the spectrum of a specific $\mathcal{N} = 4$ higher spin theory of Vasiliev that was recently analysed in detail by one of us [27]. (More specifically, this higher spin theory consists of one $\mathcal{N} = 4$ multiplet for each even spin; the fact that the leading Regge trajectory in closed string theory only consists of states (or multiplets) of even spin is also familiar from flat space, see the discussion around eq. (4.12).) For spins that are small relative to the size of the AdS space, the states on the leading Regge trajectory are described by physical states coming from the (unflowed) discrete representations of $\mathfrak{sl}(2, \mathbb{R})$; as the spin gets larger, the corresponding classical strings become longer until they hit the boundary of the AdS space where they become part of the spectrally flowed continuous representations, describing the continuum of long strings, see Figure 1.

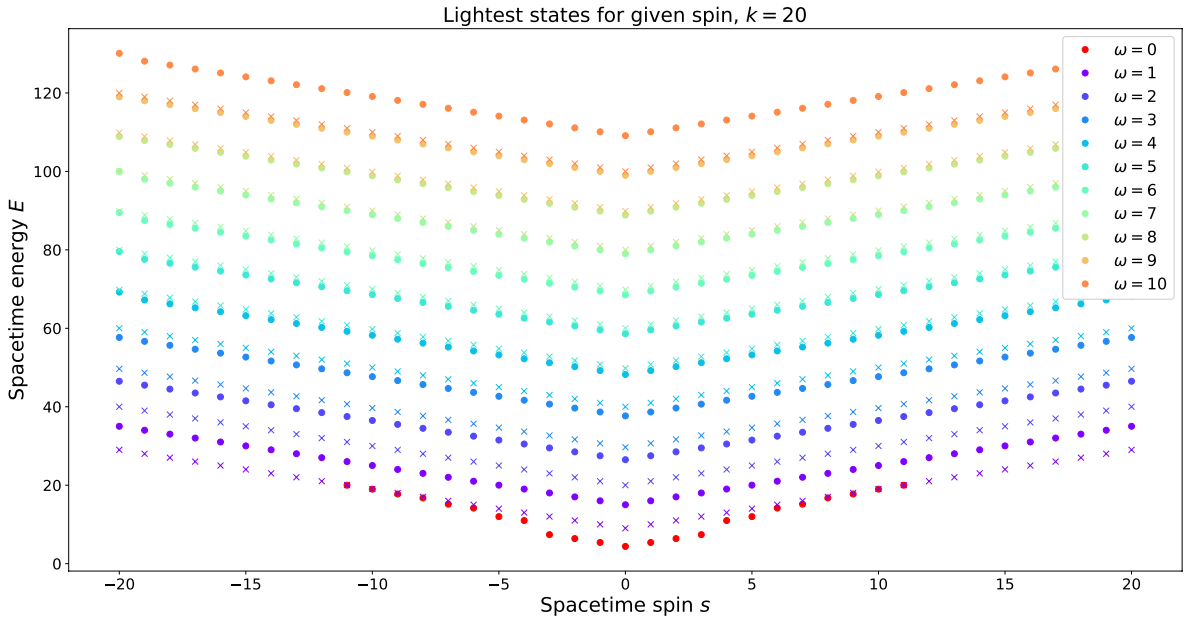


Figure 1. Lowest energy states for fixed $k = 20$ as a function of the spin s . Crosses denote continuous representations (long strings), whereas dots correspond to discrete representations. The red dots describe the unflowed discrete states, while the different bands correspond, in turn, to the flows $\omega = 1, 2, \dots, 10$. The lines corresponding to the spectrally flowed representations have been artificially capped for illustration purposes; they continue all the way to $s = \pm\infty$.

³We thank Lorenz Eberhardt for a useful discussion about this point.

This picture fits in nicely with expectations from [16–18], see also [23].

The fact that among these backgrounds with NS-NS flux no conventional higher spin symmetry emerges also has a natural interpretation in terms of the structure of the classical sigma model. Indeed, as explained in [28], the tension of the string is of the form [28, eq. (7.34)]

$$T = \sqrt{Q_{\text{NS}}^2 + g_s^2 Q_{\text{RR}}^2}, \quad (1.1)$$

where Q_{NS} and Q_{RR} are quantized, and g_s is the string coupling constant. This formula therefore suggests that the tensionless limit is only accessible in the situation with pure R-R flux (and in the limit $g_s \rightarrow 0$).

The paper is organized as follows. We explain the basics of the worldsheet theory (and set up our notation) in Section 2. In Section 3 we prove that the spectrum of this family of worldsheet theories does not contain any massless higher spin fields among the unflowed representations (describing short strings). In Section 4 we start with identifying the states that comprise the leading Regge trajectory. We first analyse the states of low spin that arise from the unflowed discrete representations. We also comment on the structure of the subleading Regge trajectory, as well as the situation for the case where \mathbb{T}^4 is replaced by K3. The rest of the leading Regge trajectory that is part of the continuous spectrum is then identified in Section 5. We also comment there on the massless higher spin fields arising from the spectrally flowed continuous representation at $k = 1$, and explain how they fit in with the expectations from [23]. Section 6 contains our conclusions, and there are three appendices where we have collected some of the more technical arguments that are referred to at various places in the body of the paper.

2 Worldsheet string theory on AdS_3

We want to study the spectrum of type IIB strings propagating on backgrounds of the form $\text{AdS}_3 \times \text{S}^3 \times X$, where X is either \mathbb{T}^4 or K3 so that the resulting theory has $\mathcal{N} = 4$ spacetime supersymmetry. We shall concentrate on the background with pure NS-NS flux for which the $\text{AdS}_3 \times \text{S}^3$ theory can be described by a (non-compact) $\text{SL}(2, \mathbb{R}) \times \text{SU}(2)$ WZW model⁴ that can be studied by conventional CFT methods. The bosonic version of this theory was discussed in some detail in the seminal papers [16–18]; in what follows we extend, following [29–32], some aspects of their analysis to the supersymmetric case.

The symmetry algebras of the supersymmetric WZW models are the $\mathcal{N} = 1$ superconformal affine algebras $\mathfrak{sl}(2, \mathbb{R})_k^{(1)} \oplus \mathfrak{su}(2)_{k'}^{(1)}$ that will be described in more detail below.

⁴Strictly speaking, we always consider the universal cover of the $\text{SL}(2, \mathbb{R})$ group, because the timelike direction of AdS_3 is taken to be non-compact.

Their central charges equal

$$c(\mathfrak{sl}(2, \mathbb{R})_k^{(1)}) = 3\left(\frac{k+2}{k} + \frac{1}{2}\right), \quad c(\mathfrak{su}(2)_{k'}^{(1)}) = 3\left(\frac{k'-2}{k'} + \frac{1}{2}\right), \quad (2.1)$$

and the condition that the total charge adds up to $c = 9$ (as befits a 6-dimensional supersymmetric background) requires then that $k = k'$. For this choice of levels, the naive $\mathcal{N} = 1$ worldsheet supersymmetry of the model is enhanced to $\mathcal{N} = 2$ [29, 33]. This enhancement can also be understood from the fact that the $\text{AdS}_3 \times \text{S}^3$ theory can be described as a non-linear sigma model on the supergroup $\text{PSL}(2|2)$ (see, e.g., [34]).

2.1 The AdS_3 WZW model

In our conventions, the $\mathfrak{sl}(2, \mathbb{R})^{(1)}$ algebra describing superstrings on AdS_3 reads

$$\begin{aligned} [J_m^+, J_n^-] &= -2J_{m+n}^3 + km\delta_{m,-n} & [J_m^3, J_n^\pm] &= \pm J_{m+n}^\pm & [J_m^3, J_n^3] &= -\frac{k}{2}m\delta_{m,-n} \\ [J_m^\pm, \psi_r^3] &= \mp \psi_{m+r}^\pm & [J_m^3, \psi_r^\pm] &= \pm \psi_{m+r}^\pm & [J_m^\pm, \psi_r^\mp] &= \mp 2\psi_{m+r}^3 \\ \{\psi_r^+, \psi_s^-\} &= k\delta_{r,-s} & \{\psi_r^3, \psi_s^3\} &= -\frac{k}{2}\delta_{r,-s}. \end{aligned} \quad (2.2)$$

The dual Coxeter number is $h_{\mathfrak{sl}(2, \mathbb{R})}^\vee = -2$. As detailed in appendix A, the shifted currents

$$\begin{aligned} \mathcal{J}^+ &= J^+ + \frac{2}{k}(\psi^3\psi^+) \\ \mathcal{J}^- &= J^- - \frac{2}{k}(\psi^3\psi^-) \\ \mathcal{J}^3 &= J^3 + \frac{1}{k}(\psi^-\psi^+) \end{aligned} \quad (2.3)$$

decouple from the fermions, $[\mathcal{J}_n^a, \psi_r^b] = 0$, and satisfy the same algebra as the J^a with level $\kappa = k + 2$. The Sugawara stress tensor and supercurrent are

$$T = \frac{1}{2k} (\mathcal{J}^+ \mathcal{J}^- + \mathcal{J}^- \mathcal{J}^+ - 2\mathcal{J}^3 \mathcal{J}^3 - \psi^+ \partial \psi^- - \psi^- \partial \psi^+ + 2\psi^3 \partial \psi^3) \quad (2.4)$$

$$G = \frac{1}{k} \left(\mathcal{J}^+ \psi^- + \mathcal{J}^- \psi^+ - 2\mathcal{J}^3 \psi^3 - \frac{2}{k} \psi^+ \psi^- \psi^3 \right), \quad (2.5)$$

where every composite operator in the above expressions is understood to be normal-ordered. These generators satisfy the $\mathcal{N} = 1$ superconformal algebra (A.17)–(A.19) with central charge (see eq. (A.20))

$$c = 3 \left(\frac{k+2}{k} + \frac{1}{2} \right). \quad (2.6)$$

The holographic dictionary implies that the global charges in the spacetime theory are given by [29]

$$L_0^{\text{CFT}} = J_0^3, \quad L_1^{\text{CFT}} = J_0^-, \quad L_{-1}^{\text{CFT}} = J_0^+, \quad (2.7)$$

with analogous expressions for the right-movers. In particular, the spacetime conformal dimension (which we henceforth refer to as the energy E) is given by the eigenvalue of $J_0^3 + \bar{J}_0^3$, while the spacetime helicity s equals $J_0^3 - \bar{J}_0^3$.⁵ Since we want to keep track of these quantum numbers, it will prove convenient to describe the representation content with respect to the coupled currents J^a .

In addition to the symmetry algebra, the actual worldsheet conformal field theory is characterised by the spectrum, i.e., by the set of $\mathfrak{sl}(2, \mathbb{R})^{(1)}$ representations that appear in the theory. For the bosonic case, a proposal for what this spectrum should be was made in [16], and the same arguments also apply here once we decouple the fermions. Recall that a highest weight representation of a (bosonic) affine Kac-Moody algebra is uniquely characterised by the representation of the zero mode algebra (in our case $\mathfrak{sl}(2, \mathbb{R})$) acting on the ‘ground states’ — these are the states that are annihilated by the modes \mathcal{J}_n^a with $n > 0$. For the case at hand, the relevant representations of $\mathfrak{sl}(2, \mathbb{R})$ that appear [16] are the so-called principal discrete representations (corresponding to short strings), as well as the principal continuous representations — together they form a complete basis of square-integrable functions on AdS_3 . Furthermore, since the no-ghost theorem truncates the set of these representations to a finite number (depending on k) [35, 36], additional representations corresponding to their spectrally flowed images appear [16]; these describe the long strings. In each case, the representation on the ground states is the same for left- and right-movers — this theory is therefore the natural analogue of the ‘charge-conjugation’ modular invariant, see also [17].

In the supersymmetric case we are interested in, we consider the above $\mathfrak{sl}(2, \mathbb{R})$ affine theory for the decoupled bosonic currents \mathcal{J}^a , and tensor to it a usual free fermion theory (where the fermions will either all be in the NS or in the R sector). Note that this will lead to a modular invariant spectrum since both factors are separately modular invariant.

In the following we shall study the spacetime spectrum of this worldsheet theory with a view towards identifying the states on the leading Regge trajectory. We shall first concentrate on the unflowed discrete representations, where the low-lying states of the leading Regge trajectory — those whose spin satisfies $s \lesssim \frac{k}{2}$ — originate from. The remaining states of the Regge trajectory are part of the continuum of long strings that is described by the (spectrally flowed) continuous representations; they will be analysed in Section 5.

2.1.1 The NS sector

In the NS sector we label the ground states by $|j, m\rangle$, where m is the eigenvalue of J_0^3 , while j labels the spin,

$$C_2|j, m\rangle = -j(j-1)|j, m\rangle, \quad J_0^3|j, m\rangle = m|j, m\rangle, \quad (2.8)$$

⁵In the following, we shall refer to s as the spin — this is what it is from the view of the two-dimensional spacetime conformal field theory.

and C_2 is the quadratic Casimir of $\mathfrak{sl}(2, \mathbb{R})$

$$C_2 = \frac{1}{2} (J_0^+ J_0^- + J_0^- J_0^+) - J_0^3 J_0^3 . \quad (2.9)$$

The condition to be ground states, i.e., to satisfy

$$J_n^a |j, m\rangle = 0 \quad \forall n \geq 1 \quad \text{and} \quad \psi_r^a |j, m\rangle = 0 \quad \forall r \geq \frac{1}{2} \quad (2.10)$$

implies, in particular, that the coupled and decoupled bosonic modes with $n \geq 0$ agree on the ground states,

$$J_n^a |j, m\rangle = \mathcal{J}_n^a |j, m\rangle , \quad n \geq 0 ; \quad (2.11)$$

the correction terms involve positive fermionic modes that annihilate the ground states. (Thus it makes no difference whether we label the ground states in terms of the decoupled or coupled spins). Furthermore, the ground states are annihilated by

$$L_n |j, m\rangle = 0 \quad \text{for } n \geq 1 \quad \text{and} \quad G_r |j, m\rangle = 0 \quad \text{for } r \geq \frac{1}{2} , \quad (2.12)$$

as follows from eqs. (2.4) and (2.5).

The discrete lowest weight representations \mathcal{D}_j^+ — in [16] they are called ‘positive energy’ — are characterised by the conditions

$$J_0^+ |j, m\rangle = |j, m+1\rangle , \quad J_0^- |j, m\rangle = \left(-j(j-1) + m(m-1) \right) |j, m-1\rangle . \quad (2.13)$$

Note that the state $|j, j\rangle$ has the lowest J_0^3 eigenvalue and is therefore annihilated by J_0^- . In particular, it follows from (2.7) that

$$\mathcal{D}_j^+ : \quad J_0^- |j, j\rangle = 0 \quad \Rightarrow \quad L_1^{\text{CFT}} |j, j\rangle = 0 \quad (2.14)$$

as appropriate for a quasiprimary state in the dual $2d$ CFT. The representation of the full affine algebra is obtained by the action of the negative modes J_{-n}^a and ψ_{-r}^a , acting on these ground states. With respect to the global $\mathfrak{sl}(2, \mathbb{R})$ algebra, all of these states will then also sit in discrete lowest weight representations of $\mathfrak{sl}(2, \mathbb{R})$, and the quasiprimary states of the dual CFT will always correspond to the lowest weight states of these discrete representations.

2.1.2 The R sector

The analysis in the Ramond sector is slightly more subtle since there are fermionic zero modes. The ground states are therefore characterised in addition by an irreducible spinor representation of the Clifford algebra in $(2+1)$ -dimensions, spanned by the fermionic zero modes — this representation is two-dimensional and can be described by $|s_0\rangle$, with $s_0 = \pm 1$. The full set of ground states is therefore labelled by $|j, m; s_0\rangle$. The presence of the fermionic zero modes implies that, unlike (2.11), the action of the decoupled and coupled bosonic zero modes differs on the ground states. In particular,

$$\mathcal{J}_0^3 = J_0^3 - \frac{1}{k} (\psi^+ \psi^-)_0 , \quad (2.15)$$

where on the ground states (see eq. (A.10))

$$(\psi^+ \psi^-)_0 |j, m; s_0\rangle = \frac{1}{2} [\psi_0^+, \psi_0^-] |j, m; s_0\rangle = k \frac{\sigma^3}{2} |j, m; s_0\rangle = k \frac{s_0}{2} |j, m; s_0\rangle, \quad (2.16)$$

and consequently

$$J_0^3 |j, m; s_0\rangle = \left(m + \frac{s_0}{2}\right) |j, m; s_0\rangle. \quad (2.17)$$

Effectively, this can be interpreted as shifting the spin j (with respect to the coupled algebra) of the R sector representation by $\pm \frac{1}{2}$ relative to the decoupled algebra.

We are interested in organising the descendants of these ground states in terms of representations of the (coupled) $\mathfrak{sl}(2, \mathbb{R})$ zero modes since they have a direct interpretation in terms of the dual CFT, see eq. (2.7). Since the creation generators — the negative bosonic and fermionic modes — transform in the adjoint representation of this $\mathfrak{sl}(2, \mathbb{R})$, the spins that arise will be of the form $j + \ell$, where j is the spin of the (decoupled) ground states while $\ell \in \mathbb{Z}$ in the NS sector and $\ell \in \mathbb{Z} + \frac{1}{2}$ in the R-sector — here we have absorbed the above shift by $\frac{1}{2}$ into the definition of ℓ . A similar consideration applies for the right-movers where the resulting spin will be $j + \bar{\ell}$ for the same j (and with the same restrictions on $\bar{\ell}$). Thus the total energy and spin of such a descendant will be

$$E = 2j + \ell + \bar{\ell}, \quad s = \ell - \bar{\ell}. \quad (2.18)$$

Note that in the NS-NS and R-R sectors the spacetime spin s will be integer, while in the NS-R and R-NS sectors it will be half-integer.

2.2 The compact directions

The remaining spacetime directions are described by $S^3 \times \mathbb{T}^4$. Supersymmetric strings propagating on S^3 can be described by a WZW model based on $\mathfrak{su}(2)^{(1)}$, for which our conventions are

$$\begin{aligned} [K_m^+, K_n^-] &= 2K_{m+n}^3 + km\delta_{m,-n} & [K_m^3, K_n^\pm] &= \pm K_{m+n}^\pm & [K_m^3, K_n^3] &= \frac{k}{2}m\delta_{m,-n} \\ [K_m^\pm, \chi_r^3] &= \mp \chi_{m+r}^\pm & [K_m^3, \chi_r^\pm] &= \pm \chi_{m+r}^\pm & [K_m^\pm, \chi_r^\mp] &= \pm 2\chi_{m+r}^3 \\ \{\chi_r^+, \chi_s^-\} &= k\delta_{r,-s} & \{\chi_r^3, \chi_s^3\} &= \frac{k}{2}\delta_{r,-s}. \end{aligned} \quad (2.19)$$

The dual Coxeter number is $h_{\mathfrak{su}(2)}^\vee = +2$. As for the case of $\mathfrak{sl}(2, \mathbb{R})^{(1)}$, we can decouple the bosons from the fermions by defining

$$\mathcal{K}^3 = K^3 - \frac{1}{k}(\chi^+ \chi^-), \quad \mathcal{K}^\pm = K^\pm \mp \frac{2}{k}(\chi^3 \chi^\pm), \quad (2.20)$$

so that $[\mathcal{K}_m^a, \chi_n^b] = 0$. The decoupled currents satisfy again the same algebra as the K^a , but with level $(k - 2)$ instead. We will therefore mostly restrict ourselves to $k \geq 2$ in this paper, see however the discussion in Section 5.1.1.⁶

The ground states of the corresponding WZW models will transform in the same representation for left- and right-movers with respect to the decoupled $\mathfrak{su}(2)$ algebras (i.e., with respect to the zero modes of (2.20)). These representations are labeled by a spin j' with $j' = 0, \frac{1}{2}, 1, \frac{3}{2}, \dots$, and their states are described by $m' = -j, -j' + 1, \dots, j' - 1, j'$, as is well-known for $\mathfrak{su}(2)$ representations. We choose the convention that the Casimir of the global decoupled algebra (i.e., of the zero modes of (2.20)) on the representation j' equals

$$\mathcal{C}_2^{\mathfrak{su}(2)} |j', m'\rangle_{S^3} = j'(j' + 1) |j', m'\rangle_{S^3} . \quad (2.21)$$

The decoupled and coupled bosonic zero modes agree in the NS-sector, while in the R-sector they differ by a fermionic contribution, and as a consequence, the K_0^3 eigenvalues in the R-sector are shifted by $\pm \frac{1}{2}$ relative to those in the NS-sector, cf., the discussion around eq. (2.17) above.

Finally, the \mathbb{T}^4 theory corresponds to four free bosons Y^i and four free fermions λ^i ($i = 1, 2, 3, 4$). The ground states in this sector are characterised by a momentum vector $|\vec{p}\rangle$ with

$$(\partial Y^i)_0 |\vec{p}\rangle = p^i |\vec{p}\rangle \quad \text{and} \quad L_0^{\mathbb{T}^4} |\vec{p}\rangle = \frac{1}{2} \sum_{i=1}^4 (p^i)^2 |\vec{p}\rangle . \quad (2.22)$$

For a compact torus the left- and right-moving momenta need not agree — they can differ by winding numbers. However, for our purposes, i.e., for identifying the leading Regge trajectory, we will always work in the zero momentum sector $\vec{p} = \vec{0}$, both for left- and right-movers. The multiplicity of the Ramond sector ground states is accounted for as usual by introducing two labels (s_2, s_3) , with $s_{2,3} = \pm$.

2.3 GSO projection

As usual in a NS-R worldsheet string theory, one must impose an appropriate GSO projection in order to remove tachyonic modes and guarantee supersymmetry of the spacetime theory. In the NS sector the worldsheet parity operator is defined to be odd on the ground states

$$(-1)^F |0\rangle_{\text{NS}} = -|0\rangle_{\text{NS}} . \quad (2.23)$$

Let us denote by N the (integer or half-integer) excitation number in the $\mathfrak{sl}(2, \mathbb{R})$ sector, while N' is the corresponding number for $\mathfrak{su}(2)$, and N'' for the \mathbb{T}^4 excitations. On a state with excitation numbers (N, N', N'') the total worldsheet parity is then

$$(-1)^F = -(-1)^{2N+2N'+2N''} . \quad (2.24)$$

⁶It is potentially interesting to study the model for certain smaller values of k such as $k = 0$, see e.g. [37, 38] and references therein for attempts in this direction (in bosonic setups). While the $k = 0$ worldsheet theory is not a standard CFT, it may be related to an integrable theory such as the principal chiral model [39, 40].

The GSO projection $(-1)^F = (-1)^{\bar{F}} = +1$ in the NS-sector thus requires that either one or all three excitation numbers are half-integer, and this has to be imposed both for left- and right-movers. In order to describe this compactly we introduce the number

$$n \equiv N + N' + N'' - \nu, \quad \text{where} \quad \nu = \begin{cases} \frac{1}{2} & \text{NS sector} \\ 0 & \text{R sector} \end{cases} \quad (2.25)$$

The above considerations imply that n has to be an integer in the NS sector, both for left- and right-movers. Obviously, the same is true in the R sector since there all excitation numbers are integers anyway.

In the R sector, the GSO projection involves also a contribution from the fermionic zero modes corresponding to $s_0 s_1 s_2 s_3$. Thus we can, for any descendant, satisfy the GSO projection by changing s_3 , if necessary. Thus the GSO projection is correctly accounted for by reducing the multiplicity of the 4-fold ground state in the R-sector of \mathbb{T}^4 — corresponding to the four choices for (s_2, s_3) with $s_{2,3} = \pm$ — to 2.

2.4 Physical state conditions

The $\mathfrak{sl}(2, \mathbb{R})$ WZW model contains a time-like direction, and as a consequence the theory is non-unitary. As usual in worldsheet string theory, the corresponding negative-norm states are removed upon imposing the Virasoro constraints. In our context, the physical state conditions are

$$L_0^{\text{tot}} - \nu = \bar{L}_0^{\text{tot}} - \bar{\nu} = 0, \quad (2.26)$$

where $\nu, \bar{\nu} = 0, \frac{1}{2}$ in the R and NS sectors, respectively, and $L_0^{\text{tot}} = L_0^{\mathfrak{sl}(2, \mathbb{R})} + L_0^{\mathfrak{su}(2)} + L_0^{\mathbb{T}^4}$. We parameterise the contributions from each component as

$$L_0^{\mathfrak{sl}(2, \mathbb{R})} = -\frac{j(j-1)}{k} + N \quad \bar{L}_0^{\mathfrak{sl}(2, \mathbb{R})} = -\frac{j(j-1)}{k} + \bar{N} \quad (2.27)$$

$$L_0^{\mathfrak{su}(2)} = \frac{j'(j'+1)}{k} + N' \quad \bar{L}_0^{\mathfrak{su}(2)} = \frac{j'(j'+1)}{k} + \bar{N}' \quad (2.28)$$

$$L_0^{\mathbb{T}^4} = h^{\mathbb{T}} + N'' \quad \bar{L}_0^{\mathbb{T}^4} = h^{\mathbb{T}} + \bar{N}'' . \quad (2.29)$$

Here, j, j' and $h^{\mathbb{T}}$ label the spins (resp. the conformal dimension) of the corresponding ground states; for the case of $\mathfrak{sl}(2, \mathbb{R})$ and $\mathfrak{su}(2)$ the relevant spins are defined with respect to the decoupled currents. Furthermore, physical states satisfy the super-Virasoro constraints

$$L_m^{\text{tot}}|\text{phys}\rangle = 0 \quad m > 0 \quad (2.30)$$

$$G_r^{\text{tot}}|\text{phys}\rangle = 0 \quad r > 0, \quad (2.31)$$

where again L^{tot} and G^{tot} denote the total worldsheet currents, receiving contributions from all three sectors of the theory.

The no-ghost theorem [35, 36, 41–43] (adapted here to the supersymmetric setup, see also [30]) shows that the Virasoro constraints (2.26) remove negative-norm states from the spectrum provided the unitarity bound

$$0 \leq j \leq \frac{k+2}{2} \quad (2.32)$$

is satisfied. This condition is the k -dependent bound on the spin j that we mentioned before, see the discussion at the end of Section 2.1. It was argued in [16], based on the structure of the spectrally flowed representations, that in fact the bound on j should be slightly stronger and take the form

$$\frac{1}{2} < j < \frac{k+1}{2} . \quad (2.33)$$

For most of the following the (weaker) unitarity bound will suffice, but for some arguments, in particular the analysis of the spectrally flowed representations, the stronger Maldacena-Ooguri (MO) bound (2.33) will be required.

Next, we write the first equation in the on-shell condition (2.26) as

$$-\frac{j(j-1)}{k} + \frac{j'(j'+1)}{k} + h^{\mathbb{T}} + n = 0 , \quad (2.34)$$

where n was defined above in eq. (2.25). In addition, we get the same equation with \bar{n} in place of n from the second condition of (2.26), where \bar{n} is defined analogously for the right-movers. We therefore conclude that $n = \bar{n}$. Furthermore, as was noted above, n is always a non-negative integer after GSO-projection. We can use eq. (2.34) to solve for j as⁷

$$j = \frac{1}{2} \left(1 + \sqrt{(2j'+1)^2 + 4k(n+h^{\mathbb{T}})} \right) . \quad (2.35)$$

Note that for fixed n , the Virasoro level of the physical states satisfy $N, N', N'' \leq n + \nu$, as follows from (2.25), and similarly in the barred sector. Since each excitation mode can raise the J_0^3 eigenvalue at most by one (and since each fermionic $\psi_{-1/2}^{\pm}$ mode can only be applied at most once), we conclude that in the NS sector the J_0^3 eigenvalue m of the physical states will lie between $j - n - 1 \leq m \leq j + n + 1$, while in the R sector it will lie between $j - n - 1/2 \leq m \leq j + n + 1/2$. This implies that the spacetime states labeled by n have spin s bounded as $|s| \leq 2n + 2$. More explicitly, the relevant states are of the form⁸

$$|j+r-n-1\rangle \otimes \overline{|j+\bar{r}-n-1\rangle}, \quad \text{with } 0 \leq r, \bar{r} \leq 2n+2 , \quad (2.36)$$

where r and \bar{r} are positive integers or zero in the NS sector, and positive half-integers in the R sector — these parameters are simply related to $(\ell, \bar{\ell})$, see the paragraph above (2.18),

⁷We have taken here the positive square root since $j > 0$ for unitarity.

⁸From what we have said so far, it is not yet clear that all these states will indeed be physical, but this will turn out to be the case, see the discussion below in Section 4. Furthermore, some of these states will appear with higher multiplicity. For the arguments of the next section it is however enough to know that only these charges can appear among the physical states.

by a shift in order to make them non-negative. The spacetime energy and spin of these states is then given by

$$E = 2j + r + \bar{r} - 2n - 2, \quad s = r - \bar{r}, \quad (2.37)$$

which in particular implies

$$E = s + 2(j + \bar{r} - n - 1). \quad (2.38)$$

Finally, it is worth pointing out how the $\text{AdS}_3 \times \text{S}^3 \times \text{T}^4$ supergravity spectrum is obtained from the worldsheet description. The supergravity states all arise for $n = 0$, which leads then to fields of spin $|s| \leq 2$. Furthermore, this condition restricts the excitation levels as $N, N', N'' \leq \nu$, and it follows that the supergravity spectrum is obtained from the level 1/2 descendants in the NS sector, as well as the R ground states. Crucially, from (2.35) (with no momentum in the T^4 directions) we deduce that the $\mathfrak{sl}(2, \mathbb{R})$ and $\mathfrak{su}(2)$ spins are related by

$$\text{SUGRA:} \quad j = j' + 1, \quad (2.39)$$

so that j is now an integer or half integer (with $j \geq 1$). We have explicitly checked that the corresponding physical states precisely reproduce the supergravity spectrum, as derived in e.g. [44]. In particular, one finds that the $j' = 0$ ($j = 1$) sector contains the (massless) graviton supermultiplet, while the representations with $j' > 0$ give rise to a tower of massive BPS multiplets.⁹

3 No massless higher spin states from short strings

With these preparations at hand we now want to analyse whether the string spectrum possesses massless higher spin states at least for some value of the level. As we shall show in this section, this will not be the case for the short strings coming from the unflowed (discrete) representations.

Recall first the standard holographic relation between the mass of an AdS_3 (bulk) excitation and the conformal dimension E and spin s of the dual operator in the boundary $2d$ CFT [45],

$$m_{\text{bulk}}^2 = (E - |s|)(E + |s| - 2), \quad (3.1)$$

where $E = h + \bar{h}$ and $s = h - \bar{h}$ in the usual CFT notation. As expected, massless higher spin fields are dual to conserved currents of dimension greater than two, which in the present context satisfy $E = |s|$ (with $|s| > 2$). Hence, massless higher spin states are characterised by the property that either the J_0^3 eigenvalue or the \bar{J}_0^3 eigenvalue vanishes.

Let us concentrate, for concreteness, on the case $\bar{J}_0^3 = 0$. Then it follows from (2.36) that we need to have

$$\text{conserved current} \quad \Rightarrow \quad j = n + 1 - \bar{r}. \quad (3.2)$$

⁹Indeed, it is easy to see from (2.38) that chiral ($E = s$) states in the $n = 0$ sector can only exist for $j = 1$ (and $\bar{r} = 0$).

Then the on-shell condition (2.34) implies that

$$k = \frac{(n - \bar{r} - j')(n + 1 - \bar{r} + j')}{n + h^{\mathbb{T}}} . \quad (3.3)$$

As discussed above, the case $n = 0$ corresponds to (supergravity) states that have $|s| \leq 2$ and are therefore not of higher spin. We may therefore assume that $n \geq 1$. Our strategy will be to show that unitarity implies that $n + \bar{r} \leq 1$, contradicting the $n \geq 1$ assumption, except for $n = 1$ and $\bar{r} = 0$. The latter case is then excluded by the stronger MO-bound (or by noticing that the relevant state is null).

First, from (3.2) we note that the unitarity bound $j \geq 0$ implies $n + 1 - \bar{r} \geq 0$. Since $j' \geq 0$ by definition, from (3.3) we find that positivity of k requires

$$\text{conserved current} + (k > 0) \quad \implies \quad n - \bar{r} > j' \geq 0 . \quad (3.4)$$

Next, we use the unitarity bound (2.32) which translates for $j = n + 1 - \bar{r}$ into

$$n - \bar{r} \leq \frac{(n - \bar{r} - j')(n + 1 - \bar{r} + j')}{2(n + h^{\mathbb{T}})} . \quad (3.5)$$

Together with (3.4), this requirement is equivalent to

$$h^{\mathbb{T}} + \frac{j'(j' + 1)}{2(n - \bar{r})} \leq \frac{1 - n - \bar{r}}{2} . \quad (3.6)$$

Since the quantity on the left hand side is greater or equal to zero (recall that $n - \bar{r} > 0$ and $h^{\mathbb{T}} \geq 0$, $j' \geq 0$ by unitarity), we conclude $n + \bar{r} \leq 1$. Finally, for $n = 1$ and $\bar{r} = 0$, we have $j = 2$, and hence from (2.35), $k \leq 2$, which is only compatible with unitarity for $k = 2$ (and incompatible with the stronger MO-bound (2.33) even in that case). Actually, the corresponding state

$$\bar{\mathcal{J}}_{-1}^- \bar{\psi}_{-1/2}^- |j = 2\rangle \quad (3.7)$$

is null at $k = 2$, as has to be the case since it saturates the unitarity bound.

Summarizing, we have shown that the only conserved currents that exist in the unflowed discrete representations appear in the supergravity spectrum ($n = 0$), and thus have spin $s \leq 2$. Our analysis holds for all values of the level $k > 0$; thus, among the WZW backgrounds there is no radius at which the theory develops a higher spin symmetry from the short string spectrum. This is in line with the arguments of the Introduction, see eq. (1.1). It is also in accord with the results of [46] where evidence was found that the symmetric orbifold point (that exhibits a large higher spin symmetry) is dual to a background with R-R flux.

The long string sector (that is described by spectrally flowed representations) will be discussed in Section 5. As we shall explain there, for $k = 1$ a stringy tower of higher spin fields appears from the spectrally flowed continuous representation, mirroring the bosonic analysis of [26]. Since these massless higher spin fields arise from long strings, they describe a qualitatively different higher spin symmetry from the usual tensionless limit [26].

4 Regge trajectories and their $\mathcal{N} = 4$ structure

Next we want to identify the leading Regge trajectory states in the string spectrum and compare this to the \mathcal{W}_∞ symmetry that was found in [7]. In order to identify the leading (and sub-leading) Regge trajectory states in the string spectrum, we first need to study in more detail the actual physical states. In this section we concentrate again on the states from the unflowed discrete representations; the spectrally flowed representations will be discussed in Section 5.

4.1 General discrete spectrum

Recall from our discussion in Section 2.4 that physical states in a representation built from an AdS_3 groundstate labeled by j take the form (2.36), with the corresponding spacetime energy and spin being given by (2.37). We now want to show that for all choices of r, \bar{r} in $0 \leq r, \bar{r} \leq 2n + 2$, physical states with these quantum numbers exist. In addition, we want to determine their multiplicities.

Let us start with some general comments about the string spectrum. One should expect that the physical states are obtained by applying eight transverse oscillators to the ground states — of the ten oscillators, one linear combination is eliminated by the Virasoro condition, and a second one leads to spurious states, i.e., gauge degrees of freedom. In the current context, it is natural to take the light-cone directions to be a linear combination of the time-like AdS_3 direction, as well as one direction on the \mathbb{T}^4 . Then the transverse (physical) excitations correspond to the \pm modes from AdS_3 , all three oscillators from the S^3 factor, and three of the four oscillators from the \mathbb{T}^4 . Thus the physical descendants of the ground states of the chiral NS and R sector are expected to be counted by — here j and j' label the spins of the $\mathfrak{sl}(2, \mathbb{R})$ and $\mathfrak{su}(2)$ ground state representation (taken with respect to the decoupled currents), respectively,¹⁰

$$\chi^{\text{NS}}(q, z, y) = q^{h(j)+h'(j')+h^{\text{T}}} \frac{y^j}{1-y} \frac{(z^{j'+1} - z^{-j'})}{(z-1)} \quad (4.1)$$

$$\times \prod_{n=1}^{\infty} \frac{(1+yq^{n-1/2})(1+y^{-1}q^{n-1/2})(1+zq^{n-1/2})(1+z^{-1}q^{n-1/2})(1+q^{n-1/2})^4}{(1-yq^n)(1-y^{-1}q^n)(1-zq^n)(1-z^{-1}q^n)(1-q^n)^4}$$

$$\chi^{\text{R}}(q, z, y) = 2q^{h(j)+h'(j')+h^{\text{T}}} \frac{y^j (y^{1/2} + y^{-1/2})}{(1-y)} \frac{(z^{j'+1} - z^{-j'})(z^{1/2} + z^{-1/2})}{(z-1)} \quad (4.2)$$

$$\times \prod_{n=1}^{\infty} \frac{(1+yq^n)(1+y^{-1}q^n)(1+zq^n)(1+z^{-1}q^n)(1+q^n)^4}{(1-yq^n)(1-y^{-1}q^n)(1-zq^n)(1-z^{-1}q^n)(1-q^n)^4}$$

¹⁰As far as we are aware, this formula was first written down in [32] generalizing the corresponding bosonic formula from [17] and building on [31]. These formulae are correct for sufficiently large values of k for which there are no non-trivial null-vectors.

where $h^{\mathbb{T}}$ is the ground state conformal dimension of the \mathbb{T}^4 theory, while for the $\mathfrak{sl}(2, \mathbb{R})$ and $\mathfrak{su}(2)$ factors we have

$$h(j) = -\frac{j(j-1)}{k}, \quad h'(j') = \frac{j'(j'+1)}{k}. \quad (4.3)$$

Here y and z are the chemical potentials with respect to $\mathfrak{sl}(2, \mathbb{R})$ and $\mathfrak{su}(2)$, respectively, and we have used that the corresponding characters are of the form

$$\chi_j(y) = \frac{y^j}{1-y}, \quad \chi_{j'}(z) = \sum_{k=-j'}^{j'} z^k = \frac{(z^{j'+1} - z^{-j'})}{(z-1)}. \quad (4.4)$$

Furthermore, q keeps track of the total Virasoro eigenvalue which has to equal q^ν for the actual physical states, see eq. (2.26). (We are here describing one chiral sector; the results for left- and right-movers then has to be combined.) The first line in each of (4.1)-(4.2) accounts for the contribution of the ground state representations, while the second line describes the contributions of the non-zero oscillators. The overall multiplicity of 2 in the R-sector reflects the overall multiplicity after GSO projection, see the discussion after eq. (2.25).

We have checked this prediction in some detail (by solving the physical state conditions explicitly, at least for some low-lying states), and we have found complete agreement. We should mention, though, that there are some subtleties with the counting for $j = 1$; this is discussed in more detail in Appendix B.

We note that this formula in particular implies that, for all $0 \leq r \leq 2n + 2$, physical states with these quantum numbers exist. In order to see this, we solve for j (in terms of n , j' and $h^{\mathbb{T}}$) using eq. (2.35); then the overall power of q^ν comes from taking the term with $q^{n+\nu}$ from the oscillator product in the second line. In the NS sector $r = 0$ then corresponds to the situation where the J_0^3 eigenvalue is $j - n - 1$. This can be achieved by taking from the numerator the term $y^{-1}q^{1/2}$, as well as n powers of $y^{-1}q^1$ from the geometric series expansion of the denominator term $(1 - y^{-1}q)$. The corresponding state is thus of the form

$$|j - n - 1\rangle = (\mathcal{J}_{-1}^-)^n \psi_{-1/2}^- |j\rangle. \quad (4.5)$$

Similarly, the case $r = 2n + 2$ corresponds to having J_0^3 eigenvalue $j + n + 1$, in which case the relevant powers are $yq^{1/2}$ from the numerator, and n powers of yq^1 from the geometric series expansion of the denominator term $(1 - yq)$. Schematically, the corresponding state is thus of the form

$$|j + n + 1\rangle = \left[(\mathcal{J}_{-1}^+)^n \psi_{-1/2}^+ |j\rangle + \dots \right], \quad (4.6)$$

where the dots stand for additional terms that make it a lowest weight state with respect to the $\mathfrak{sl}(2, \mathbb{R})$ algebra. In either case it is easy to see that these representations appear with multiplicity one — these are the ‘extremal’ cases that can only be obtained in one way.

On the other hand, the intermediate cases $0 < r < 2n + 2$ can be obtained in more than one way, but from the above analysis it is clear that all of these terms will indeed arise.

Incidentally, we should note that it follows from the explicit formula that (apart from the overall $y^j/(1-y)$ term) the partition function is symmetric under the symmetry $y \leftrightarrow y^{-1}$. As a consequence, the multiplicities of the representations corresponding to r and $2n+2-r$ will be the same.

Combining left- and right-movers, the full spacetime spectrum (in terms of energy and spin) forms a diamond in the (E, s) plane for fixed n , depicted in Figure 2. Here the corner points have multiplicity one, but the other points have higher multiplicity.

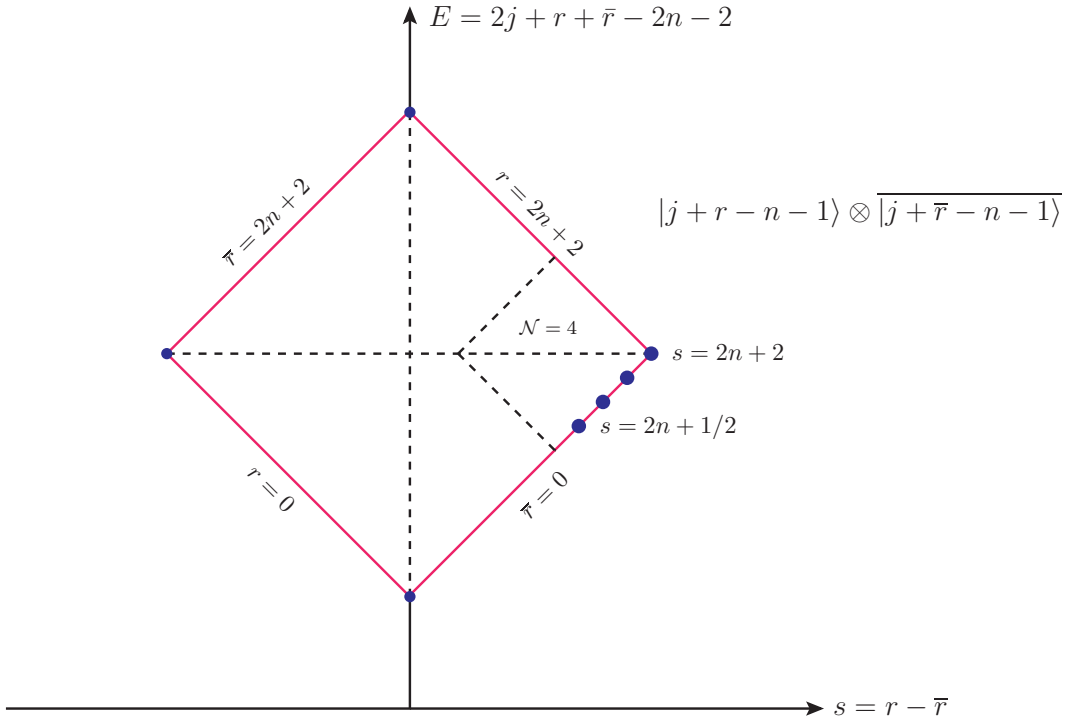


Figure 2. Schematic description of the discrete physical spectrum for fixed n (and fixed j). The four blue dots on the $\bar{r} = 0$ edge denote the top component of supermultiplets with the lowest energy for the given spin. See section 4.2 below for a detailed discussion of these states.

On general grounds it is clear that we must be able to organise the spectrum in terms of (small) $\mathcal{N} = (4, 4)$ representations, see Appendix C for a brief review of their structure. In the (E, s) plane, $\mathcal{N} = (4, 4)$ multiplets form small diamonds with edges spanning two units of energy and two units of spin. For example, the right most vertex of the diamond in Figure 2, which is characterised by $(r, \bar{r}) = (2n+2, 0)$, has multiplicity one (since both r and \bar{r} take their extremal values), and corresponds to the chiral states with $h = j + n + 1$ and $\bar{h} = j - n - 1$. This state is then the top ($h = h_0 + 2$) component of the left-moving long $\mathcal{N} = 4$ multiplet whose bottom component has $h_0 = j + n - 1$ and transforms in the

representation \mathbf{m} of $\mathfrak{su}(2)$, where $m = 2j' + 1$, see Table 6 of Appendix C. Similarly, with respect to the right-movers, the state is the bottom component of a similar $\mathcal{N} = 4$ multiplet with $\bar{h}_0 = j - n - 1$. The relevant states in the full multiplet then give rise to states in the dashed diamond in Figure 2. (Here we have also included the R sector states that are needed to complete the multiplets.)

Once the states that sit in this multiplet have been accounted for, we look at the remaining states and proceed iteratively. For example, the ‘extremal’ R sector states that contribute to this multiplet have $h = j + n + \frac{1}{2}$ and/or $\bar{h} = j - n - \frac{1}{2}$. Concentrating on the first case, it follows from (4.2) that there will be $8m$ states of this form transforming as $4 \cdot (\mathbf{m} + 1)$ and $4 \cdot (\mathbf{m} - 1)$ — one factor of 2 is the overall factor in eq. (4.2), while the other factor of 2 comes from the fact that we can either use one fermionic (-1) mode in the R-sector or none. Furthermore, the two different representations come from tensoring with the spin $\frac{1}{2}$ representation described by the factor $(z^{1/2} + z^{-1/2})$ in the first line. Two copies of each of these two representations are part of the long $\mathcal{N} = 4$ multiplet, see Table 6, while the other two will generate two pairs of new $\mathcal{N} = (4, 4)$ multiplets, whose bottom components will transform as $(\mathbf{m} + 1)$ and $(\mathbf{m} - 1)$, respectively. (The second dot along the $\bar{r} = 0$ edge in Figure 2 represents states in these multiplets.) Proceeding in this manner, we find that the multiplicity of the $\mathcal{N} = 4$ multiplets along the $\bar{r} = 0$ edge (i.e., only considering states whose bottom component is $\bar{h}_0 = j - n - 1$) is described in Table 1.

s	$\delta m = -5$	-4	-3	-2	-1	0	1	2	3	4	5
$2n + 2$						1					
$2n + 3/2$					2		2				
$2n + 1$				2		9		2			
$2n + 1/2$			2		18		18		2		
$2n$		2		23		61		23		2	
$2n - 1/2$	2		24		116		116		24		2
...

Table 1. Multiplicity of the $\mathcal{N} = 4$ multiplets that arise along the $\bar{r} = 0$ edge for the case where j' and hence \mathbf{m} is sufficiently big. Here and below the spin always refers to the spin s of the ‘top’ component of the $\mathcal{N} = 4$ multiplet — the bottom component then has spin $s - 2$.

For future reference, in Table 2 we also give the multiplicity of the $\mathcal{N} = 4$ multiplets along the $\bar{r} = 0$ edge for $j' = 0$, i.e., $\mathbf{m} = 1$ — in this case, only $\delta m \geq 0$ is possible and some of the multiplicities are reduced.

4.2 Leading Regge trajectory

Having discussed the general structure of the discrete string spectrum, we can now identify the states on the leading Regge trajectory. These are the states that should have the lowest energy for a given spin, together with their $\mathcal{N} = (4, 4)$ descendants. We want to argue that they are precisely described by the dashed diamond in Figure 2, where n takes the values $n = 0$, $n = 1$, $n = 2$, etc.

	1	2	3	4	5	6	...
$2n + 2$	1						
$2n + 3/2$		2					
$2n + 1$	7		2				
$2n + 1/2$		16		2			
$2n$	38		21		2		
$2n - 1/2$		92		22		2	
...

Table 2. Multiplicities of $\mathcal{N} = 4$ multiplets along the $\bar{r} = 0$ edge for $j' = 0$, i.e., $\mathbf{m} = 1$.

First we note that the leading Regge trajectory states will be associated to states with $j' = 0$ (and $h^{\mathbb{T}} = 0$) — for fixed n , as well as (r, \bar{r}) , the choice of j' and $h^{\mathbb{T}}$ only enters via j as defined in (2.35), and j in turn only contributes to E , but not to s , see eq. (2.37). Choosing j' and or $h^{\mathbb{T}}$ to be non-trivial, increases j and hence E , but does not modify the spin s . The states of lowest energy (for fixed spin) therefore arise for $j' = h^{\mathbb{T}} = 0$.

Similarly, by construction, the states with lowest energy for given spin lie (for fixed n and hence j — recall that $j' = h^{\mathbb{T}} = 0$) on the lower edges of the representation diamond. Without loss of generality, focusing on positive helicity modes we can then restrict our attention to the $\bar{r} = 0$ edge. The energies of these states satisfy the linear dispersion relation

$$E_{\text{Regge}}(s) = s - 2n - 1 + \sqrt{1 + 4kn} , \quad 2n < s \leq 2n + 2 , \quad (4.7)$$

where the inequality $2n < s$ arises because the lowest energy state with spin $s = 2n$ is obtained from the diamond corresponding to $\tilde{n} = n - 1$ — this is a consequence of the inequality

$$\sqrt{1 + 4kn} \geq 2 + \sqrt{1 + 4k(n - 1)} , \quad (4.8)$$

which, after squaring twice, is equivalent to

$$(k + 2) \geq 4n ; \quad (4.9)$$

in turn this follows from the unitarity bound, see eq. (2.32), using the expression for j from eq. (2.35) with $j' = h^{\mathbb{T}} = 0$. The conformal dimensions of the leading Regge trajectory states for small values of the spin are plotted (for $k = 200$) in Figure 3.

As a side remark, we should note that the states with dispersion relation (4.7) formally become chiral if k takes the value $k = n + 1$. However, this choice is not allowed by the unitarity bound, except for the supergravity states with $n = 0$ and the special solution $n = 1$ that was already discussed after eq. (3.6). [The latter case corresponds to $n = 1$ and $k = 2$ and is incompatible with the MO bound (2.33).]

Since $\bar{r} = 0$ the right-moving states are the ‘extremal’ states with $\bar{N}' = \bar{N}'' = 0$, so that the right-moving (barred) $\mathfrak{su}(2)$ representation is always trivial. Furthermore, the leading term with $r = 2n + 2$ is also trivial with respect to the left-moving $\mathfrak{su}(2)$ algebra, and it is the top state of an $\mathcal{N} = (4, 4)$ multiplet with $\mathfrak{su}(2) \oplus \mathfrak{su}(2)$ quantum numbers $(\mathbf{1}, \mathbf{1})$.

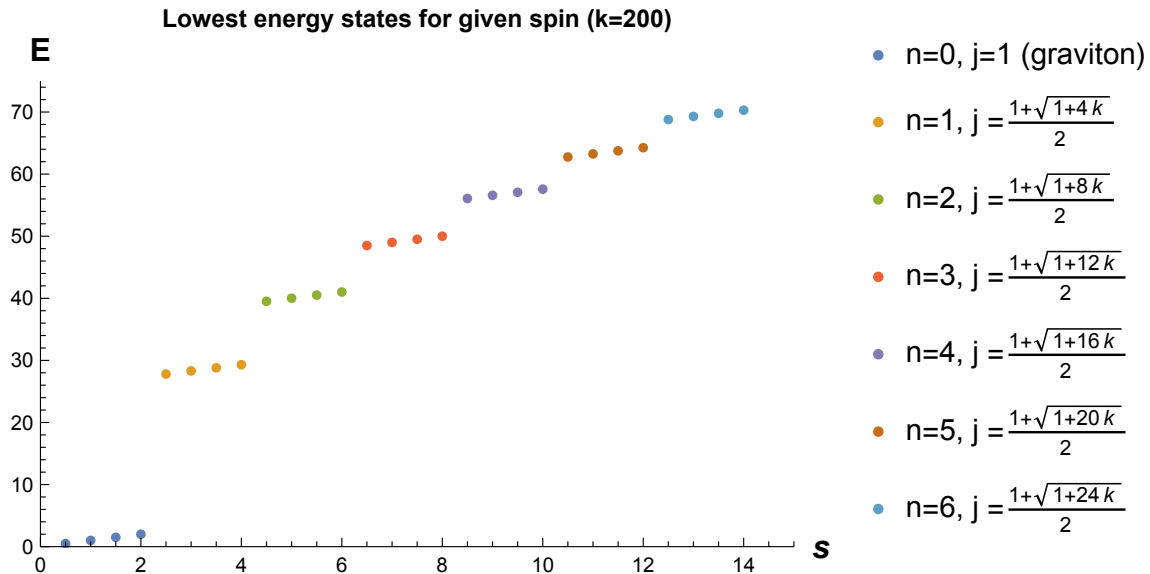


Figure 3. Dispersion relation of the lowest energy states for $k = 200$. The dots correspond to the set of four states singled out in Figure 2, depicted here for different values of n (i.e. different j), giving rise to different ranges $2n + 1/2 \leq s \leq 2n + 2$ of the spin. In each family of four dots, the last one describes a unique state, the corner state of Figure 2, while the first three correspond to states with higher multiplicity.

We now want to argue that the leading Regge trajectory consists just of the first multiplet of Table 2 for each n . This is natural since there is only a single multiplet with these quantum numbers; its top component is obtained by tensoring the $\mathfrak{sl}(2, \mathbb{R})$ representations (4.5) and (4.6) for the left- and right-moving sector, respectively. (The terms with $r < 2n + 2$, on the other hand, lead in general to $\mathcal{N} = (4, 4)$ multiplets for which the left-moving $\mathfrak{su}(2)$ spin is not trivial.) Furthermore, these states always define the states with smallest energy for the given spin, independent of k .¹¹ In order to see this, it is enough to show that $E(n, s = 2n + 2) < E(p, s = 2n + 2)$ for any $p > n$ — note that a state with this spin can only appear for $p \geq n$. Without loss of generality it is enough to concentrate on the case $p = n + 1$ since any $p > n$ can be iteratively obtained in this manner. Furthermore, we may assume that the relevant state in the p 'th (i.e., $n + 1$ 'th) diamond sits on the lower edge, i.e., has energy described by eq. (4.7). Then the inequality we need to prove is simply

$$\sqrt{1 + 4kp} \geq \sqrt{1 + 4k(p - 1)} + 2, \quad (4.10)$$

which upon squaring both sides (after subtracting 2) leads to

$$1 + k \geq \sqrt{1 + 4kp}. \quad (4.11)$$

This identity is now a direct consequence of the unitarity bound, see eq. (4.9) with $n = p$.

¹¹The situation is in general more complicated for the other states, see the discussion of the next subsection.

We note that these states carry exactly the same quantum numbers as the generators of the even spin $\mathcal{N} = 4$ \mathcal{W}_∞ algebra that was analysed in [27]. This is the minimal version of the $\mathcal{N} = 4$ higher spin symmetry, and it has a nice AdS_3 dual that is also discussed in some detail in [27]. On the other hand, while the string spectrum also contains multiplets with odd integer spin, there does not seem to be any natural candidate for which of the 7 singlet multiplets at spin $2n + 1$, see Table 2, should be added to the even spin \mathcal{W}_∞ algebra in order to generate the full $\mathcal{N} = 4$ \mathcal{W}_∞ algebra of [7] (or the extended algebra of [46] where also the charged bilinears are included in the higher spin algebra). Incidentally, the fact that the leading Regge trajectory should only be identified with the fields (or multiplets) of even spin is also expected from bosonic closed string theory in flat space. There the states of the leading Regge trajectory are associated to the worldsheet states of the form

$$\alpha_{-1}^{\mu_1} \cdots \alpha_{-1}^{\mu_n} \bar{\alpha}_{-1}^{\nu_1} \cdots \bar{\alpha}_{-1}^{\nu_n} |p\rangle, \quad (4.12)$$

where the level-matching condition requires that the number of transverse oscillators on the left and right is the same. As a consequence, this only leads to fields of even spin $s = 2n$.

4.3 Subleading $\mathcal{N} = 4$ trajectory

Unlike the leading Regge trajectory, the identification of the subleading trajectory turns out to be somewhat less clean, and in particular it depends on the value of k . For $2n < s \leq 2n+2$ there are a priori three kinds of states competing to be the subleading trajectory. These are the states in the interior of the $(n, j' = 0)$ diamond; the states on edge of the $(n, j' = 1/2)$ diamond; and the states on the edge of the $(n+1, j' = 0)$ diamond. Denoting the energies of these three sets by $E_n^*(j' = 0)$, $E_n(j' = 1/2)$, and $E_{n+1}(j' = 0)$, respectively, we find that their explicit values for the relevant spins are as given in Table 3.

s	$E_n^*(j' = 0)$	$E_{n+1}(j' = 0)$	$E_n(j' = 1/2)$
$2n + 2$	-	$-1 + \sqrt{1 + 4k(n+1)}$	$1 + 2\sqrt{1 + kn}$
$2n + 3/2$	$\frac{3}{2} + \sqrt{1 + 4kn}$	$-\frac{3}{2} + \sqrt{1 + 4k(n+1)}$	$\frac{1}{2} + 2\sqrt{1 + kn}$
$2n + 1$	$1 + \sqrt{1 + 4kn}$	$-2 + \sqrt{1 + 4k(n+1)}$	$2\sqrt{1 + kn}$
$2n + 1/2$	$\frac{1}{2} + \sqrt{1 + 4kn}$	$-\frac{5}{2} + \sqrt{1 + 4k(n+1)}$	$-\frac{1}{2} + 2\sqrt{1 + kn}$

Table 3. Candidates for subleading Regge trajectory with $2n < s \leq 2n + 2$.

It turns out that among these states, the one with the smallest energy is

$$E_{n+1}(j' = 0) \quad \text{if} \quad k \leq k_n^* = \frac{7}{4} + 2n + \sqrt{4n^2 + 7n + 4} \quad (4.13)$$

$$E_n(j' = 1/2) \quad \text{if} \quad k \geq k_n^* = \frac{7}{4} + 2n + \sqrt{4n^2 + 7n + 4}. \quad (4.14)$$

A few remarks are in order. First, the competing states always lie on the edge of some diamond. Second, for fixed k , the choice between the two diamonds is n - and therefore s -dependent. Nevertheless, the existence of a minimum value for n (which is $n = 0$) implies

that we can make the states of eq. (4.13) to be the subleading ones for all possible values of n , and thus for all higher spin states, by tuning k to be small enough. This happens for $k \leq \frac{15}{4}$. Note that since k must be integer, this allows for the two solutions $k = 2$ and $k = 3$.

We should also note that the $\mathfrak{su}(2) \oplus \mathfrak{su}(2)$ quantum numbers are different for these two sets of competing representations, as detailed in Table 4. In particular, the states of the second column are non-trivial with respect to the right-moving $\mathfrak{su}(2)$ algebra. Unfortunately, there does not seem to be any particularly simple pattern among these representations, and they do not seem to be naturally in correspondence with the subleading Regge trajectory of [46].¹² Obviously, there is no fundamental reason why such a correspondence should exist — the two descriptions refer to different points in moduli space.

s	$k < k_n^*$	$k > k_n^*$
$2n + 2$	$2 \cdot (\mathbf{5}, \mathbf{1}) \oplus 21 \cdot (\mathbf{3}, \mathbf{1}) \oplus 38 \cdot (\mathbf{1}, \mathbf{1})$	$(\mathbf{2}, \mathbf{2})$
$2n + 3/2$	$2 \cdot (\mathbf{6}, \mathbf{1}) \oplus 26 \cdot (\mathbf{4}, \mathbf{1}) \oplus 88 \cdot (\mathbf{2}, \mathbf{1})$	$2 \cdot (\mathbf{3}, \mathbf{2}) \oplus 2 \cdot (\mathbf{1}, \mathbf{2})$
$2n + 1$	$2 \cdot (\mathbf{7}, \mathbf{1}) \oplus \dots$	$2 \cdot (\mathbf{4}, \mathbf{2}) \oplus 9 \cdot (\mathbf{2}, \mathbf{2})$
$2n + 1/2$	$2 \cdot (\mathbf{8}, \mathbf{1}) \oplus \dots$	$2 \cdot (\mathbf{5}, \mathbf{2}) \oplus 18 \cdot (\mathbf{3}, \mathbf{2}) \oplus 16 \cdot (\mathbf{1}, \mathbf{2})$

Table 4. States composing the subleading $\mathcal{N} = 4$ trajectory for different values of k .

4.4 $\text{AdS}_3 \times \text{S}^3 \times \text{K3}$

One may hope that the situation could become a bit simpler for the case of $\text{AdS}_3 \times \text{S}^3 \times \text{K3}$, since then the spectrum will contain fewer states. Let us consider the case when K3 can be described as a $\mathbb{T}^4/\mathbb{Z}_2$ orbifold. This \mathbb{Z}_2 orbifold can be easily implemented in the worldsheet description since it simply acts as a minus sign on each of the four bosonic and fermionic oscillators associated to the \mathbb{T}^4 . For each n , the surviving states organise themselves into $\mathcal{N} = 4$ multiplets as

s	$\delta m = -5$	-4	-3	-2	-1	0	1	2	3	4	5
$2n + 2$						1					
$2n + 3/2$					0		0				
$2n + 1$				2		5		2			
$2n + 1/2$			0		10		10		0		
$2n$		2		11		29		11		2	
$2n - 1/2$	0		12		56		56		12		0
\dots	\dots	\dots	\dots	\dots	\dots	\dots	\dots	\dots	\dots	\dots	\dots

Table 5. Number of the \mathbb{Z}_2 -even $\mathcal{N} = 4$ multiplets for $\bar{r} = 0$ organized by their $\mathfrak{su}(2)$ quantum numbers. This is to be compared to Table 1.

¹²We should mention that among the above states one should expect that some do not become chiral at the symmetric orbifold point, i.e., do not belong to the stringy higher spin symmetry, but remain massive even at that point in moduli space.

Unfortunately, there is still a fairly large multiplicity (namely $3 = 5 - 2$ — the subtraction of 2 arises as in the passage from Table 1 to Table 2) for the first odd spin ‘leading’ Regge trajectory states, and again the most natural interpretation is that the leading Regge trajectory has just even spin multiplets as before. Similarly, the situation for the subleading Regge trajectory also does not seem to improve significantly.

5 Spectrally flowed sectors and long strings

In the previous section we have identified the low-lying states of the leading Regge trajectory that originate from the unflowed discrete representations. More specifically, these states have spin $s = 2n + 2$, with $n = 0, 1, 2, \dots, \frac{1}{4}(k + 2)$, where the upper bound comes from eq. (4.9), which in turn is a consequence of the unitarity bound (2.32). If we impose the slightly stronger MO-bound (2.33), we find instead

$$s < \frac{k}{2} + 2 - \frac{1}{2k} . \quad (5.1)$$

In either case, we only get finitely many states in this manner. In this section we look for the remaining states of the leading Regge trajectory. As we shall see, they arise from the continuous representations describing long strings. This makes also intuitive sense since the leading Regge trajectory states correspond to longer and longer strings that get closer to the boundary of AdS_3 , until they finally merge with the continuum of long strings.

We start by describing the rest of the full string spectrum that corresponds to the spectrally flowed continuous and discrete representations. For each class of representation we then identify the states of lowest mass for a given spin. We will see that the states from the unflowed discrete representations are indeed the lightest states of a given spin for small spin; furthermore, for $s \approx \frac{k}{2}$, the spectrally flowed continuous representations will take over.

The spectrally flowed representations are obtained from the discrete and continuous representations upon applying the automorphism of $\mathfrak{sl}(2, \mathbb{R})^{(1)}$ defined by

$$\begin{aligned} \tilde{J}_n^3 &= J_n^3 + \frac{k}{2}\omega\delta_{n,0} \\ \tilde{J}_n^\pm &= J_{n\mp\omega}^\pm \\ \tilde{\psi}_r^3 &= \psi_r^3 \\ \tilde{\psi}_r^\pm &= \psi_{r\mp\omega}^\pm \\ \tilde{L}_n &= L_n - \omega J_n^3 - \frac{k}{4}\omega^2\delta_{n,0} . \end{aligned} \quad (5.2)$$

Here ω is an integer, and the same automorphism (with the same value of ω) is applied to both left- and right-movers. We characterise the spectrally flowed representations by using the same underlying vector space, but letting the \tilde{J}_m^a modes act on it (rather than the J_m^a modes), and similarly for the fermions. In order for the resulting representation to decompose into lowest weight representations of $\mathfrak{sl}(2, \mathbb{R})$ we need, in particular, that

$$\tilde{J}_0^- |j, m\rangle = J_\omega^- |j, m\rangle = 0 . \quad (5.3)$$

Thus we take ω to be a positive integer (or zero). Note that the \tilde{J}_0^3 eigenvalue of the states is then

$$\tilde{J}_0^3 |j, m\rangle = \left(m + \frac{k}{2}\omega\right) |j, m\rangle, \quad (5.4)$$

where m is the actual J_0^3 eigenvalue of the state in question. Since ω is positive, this eigenvalue is always positive (at least on the ground states).

Using the explicit form of \tilde{L}_0 (c.f. (5.2)), the on-shell condition is in the NS-sector and for general ω

$$-\frac{j(j-1)}{k} - \omega \left(m + \frac{k}{4}\omega\right) + N_{\text{tot}} = \frac{1}{2}, \quad (5.5)$$

where $N_{\text{tot}} = N + N' + N''$ is the total excitation number, and we have set $j' = h^{\text{T}} = 0$. A similar condition also applies to the right-movers, and we have the level-matching condition

$$N_{\text{tot}} - \bar{N}_{\text{tot}} = \omega s \quad (5.6)$$

since (5.5) involves the term ωm . Finally, we need to impose the GSO-projection. It is natural to assume — and this leads to the correct BPS spectrum of [47] — that the correct GSO projection is the one that takes the same form in all representations, including the spectrally flowed ones. In terms of the original vector space description we are using here, this then translates into the condition

$$N_{\text{tot}} + \frac{\omega + 1}{2} \in \mathbb{N}, \quad (5.7)$$

since we only flow in the $\mathfrak{sl}(2, \mathbb{R})$ factor and hence the fermion number of the ground state changes by one for each unit spectral flow, see also [48].¹³

5.1 Spectrally flowed representations — the continuous case

According to [16] the spectrum of string theory on AdS_3 contains representations whose ground states transform in continuous representations of $\mathfrak{sl}(2, \mathbb{R})$. The states of the continuous representation \mathcal{C}_j^α are labelled by $|j, m, \alpha\rangle$, where $j = \frac{1}{2} + ip$ with p real, and m takes all values of the form $m = \alpha + \mathbb{Z}$. These representations are neither highest nor lowest weight with respect to $\mathfrak{sl}(2, \mathbb{R})$. Their Casimir is given by

$$C_2 |j, m, \alpha\rangle = -j(j-1) |j, m, \alpha\rangle, \quad -j(j-1) = \frac{1}{4} + p^2. \quad (5.8)$$

In particular, they can therefore only satisfy the mass-shell condition (2.26) in the NS-sector with $N_{\text{tot}} = \bar{N}_{\text{tot}} = 0$. Since this is incompatible with the GSO projection, there are no physical states in the *unflowed* continuous representations.¹⁴ However, after spectral flow, these representations give rise to interesting physical states, as we shall now describe.

¹³There is a similar spectral flow automorphism for $\mathfrak{su}(2)^{(1)}$, but since this does not lead to new representations, it is a matter of convenience whether we include this flow or not. In our context, it is simpler not to flow in this sector.

¹⁴This should better be so, since otherwise the dual CFT would have had an unbounded L_0 spectrum.

Because of (5.3) (applied to $|j, m, \alpha\rangle$) the spectrally flowed continuous representations are lowest weight with respect to $\mathfrak{sl}(2, \mathbb{R})$ if $\omega > 0$. Plugging $j = \frac{1}{2} + ip$ into the mass-shell condition (5.5) and solving for m leads to

$$m = -\frac{k\omega}{4} + \frac{1}{\omega} \left(N_{\text{tot}} - \frac{1}{2} + \frac{p^2}{k} + \frac{1}{4k} \right), \quad (5.9)$$

and similarly for \bar{m} . (Remember that j , i.e., p , and ω are the same for both left- and right-moving representations.) Using (5.4) the spacetime energy of the state is then

$$E_{\text{cont}} = m + \frac{k\omega}{2} + \bar{m} + \frac{k\omega}{2} = \frac{k\omega}{2} + \frac{1}{\omega} \left(N_{\text{tot}} + \bar{N}_{\text{tot}} - 1 + \frac{2p^2}{k} + \frac{1}{2k} \right). \quad (5.10)$$

It is clear that the lowest energy for any given quantum numbers is achieved by putting $p = 0$, as also expected classically. Furthermore, using level-matching (5.6) to solve for the spin we can rewrite this as

$$E_{\text{cont}}(s) = s + \frac{k\omega}{2} + \frac{1}{\omega} \left(2\bar{N}_{\text{tot}} + \frac{1}{2k} - 1 \right). \quad (5.11)$$

Thus the minimum energy for a given s is achieved by putting $\bar{N}_{\text{tot}} = 0$ if ω is odd, or $\bar{N}_{\text{tot}} = 1/2$ if ω is even (as required by the GSO projection, eq. (5.7)). For any $k > \sqrt{6}/2 - 1 \simeq 0.22$ and any even $\omega \geq 2$, the continuous $(\omega - 1)$ sector has lower energy. Hence, in what follows we focus on the case of odd ω . Since $\omega s = N_{\text{tot}}$, with $\omega \geq 1$, setting $\bar{N}_{\text{tot}} = 0$ is only valid for $s \geq 0$. (Analogously, the lowest energy for $s \leq 0$ is achieved by putting $N_{\text{tot}} = 0$, so that $\omega s = -\bar{N}_{\text{tot}}$.) Thus we conclude that the spectrally flowed continuous representations contain states with the dispersion relation

$$E_{\text{cont}}(s) = |s| + \frac{k\omega}{2} + \frac{1}{\omega} \left(\frac{1}{2k} - 1 \right) \quad (\omega \text{ odd}) \quad (5.12)$$

for any spin s . This energy is a growing function of $\omega \in \mathbb{N}$ for any $k > -1 + \sqrt{2} \simeq 0.41$. Since there is no constraint on the set of spins, the lowest energy for any spin is achieved by putting $\omega = 1$, for which we then find

$$E_{\text{cont}}(s) = |s| + \frac{k}{2} + \frac{1}{2k} - 1. \quad (5.13)$$

5.1.1 Massless higher spin fields for $k = 1$

We should note that for $k = 1$, (5.13) describes massless higher spin states. For this value ($k = \omega = 1$), the mass-shell condition (5.9) (and its right-moving analogue) become simply

$$m = N_{\text{tot}} - \frac{1}{2}, \quad \bar{m} = \bar{N}_{\text{tot}} - \frac{1}{2}, \quad (5.14)$$

while the conformal dimensions of the dual CFT are

$$h = m + \frac{1}{2} = N_{\text{tot}}, \quad \bar{h} = \bar{m} + \frac{1}{2} = \bar{N}_{\text{tot}}, \quad (5.15)$$

and the GSO-projection (5.7) requires now that both N_{tot} and \bar{N}_{tot} should be integers. Since there are eight transverse oscillators, there is a stringy growth of massless higher spin fields.

This phenomenon is the exact analogue of what was found for the bosonic case, where the corresponding phenomenon happens for $k_{\text{bos}} = 1 + 2 = 3$ in [26]. (In particular, $k = 1$ is also the minimum value where the massless graviton that arises from the discrete representation with $j = 1$ is allowed by the MO-bound (2.33).) The theory with $k = 1$ describes strings scattering off a single NS5 brane; while this is formally an ill-defined theory — the level of the bosonic $\mathfrak{su}(2)$ algebra is negative, $k'_{\text{bos}} = 1 - 2 = -1$, although this conclusion could be avoided if we consider instead of $\text{AdS}_3 \times \text{S}^3 \times \mathbb{T}^4$ the background $\text{AdS}_3 \times \text{S}^3 \times \text{S}^3 \times \text{S}^1$, see the comments at the bottom of page 2 — it was argued in [23] that at least some aspects of the theory still make sense. Note that the gap of the spectrum was predicted in [23] to be

$$\Delta_0 = \frac{(k-1)^2}{4k}, \quad (5.16)$$

see eq. (4.26) of [23], and this is reproduced exactly (as in the bosonic case of [26]) in our analysis from the mass-shell condition (5.9) for $p = 0$, $w = 1$ and $N_{\text{tot}} = 0$. It was furthermore argued there that the dual CFT should correspond to a symmetric orbifold associated to $\mathbb{R}^4 \times \mathbb{T}^4$. (Here the \mathbb{R}^4 arises from the S^3 together with the radial direction of AdS_3 that becomes effectively non-compact in this limit.) This is nicely in line with our finding of the massless higher spin fields. In particular, given that the symmetric orbifold involves an 8-dimensional free theory, the single particle generators have the same growth behaviour as found above in (5.15), see [49, 50].

On the other hand, this tensionless limit is different in nature to what one expects from the symmetric orbifold of \mathbb{T}^4 , see [26] for a discussion of this point. In particular, one may expect that these massless higher spin states get lifted upon switching on R-R flux. It would be interesting to confirm this, using the techniques of [28].

5.2 Spectrally flowed representations — the discrete case

For discrete flowed representations, it follows from the analysis of [16] that j satisfies the MO-bound

$$\frac{1}{2} < j < \frac{k+1}{2}. \quad (5.17)$$

Writing $m = j + r$, and solving the on-shell condition (5.5) for j , we find

$$j = \frac{1}{2} \left[1 - k\omega + \sqrt{1 + 4k \left(N_{\text{tot}} - r\omega - \frac{\omega + 1}{4} \right)} \right]. \quad (5.18)$$

In addition, we must solve the constraints $r \geq -N$ for ω odd, and $r \geq -N - 1/2$ for ω even. We should note that $\omega s = N_{\text{tot}} - \bar{N}_{\text{tot}}$, and $s = r - \bar{r}$, so that $N_{\text{tot}} - r\omega = \bar{N}_{\text{tot}} - \bar{r}\omega$. Then j is indeed the same for the left- and right-moving sectors.

We first note that j is a decreasing function of r . The unitarity constraint $j \geq 0$, together with the fact that there is a minimum value that r can take as a function of N , leads to the existence of a minimum value for the levels $N_{\text{tot}}, \bar{N}_{\text{tot}}$ in a given ω sector, which is of the form

$$\omega \text{ odd: } \quad N_{\text{tot}}, \bar{N}_{\text{tot}} \geq \frac{k\omega^2 + 2}{4\omega + 4} \quad (5.19)$$

$$\omega \text{ even: } \quad N_{\text{tot}}, \bar{N}_{\text{tot}} \geq \frac{k\omega^2 + 2}{4\omega + 4} - \frac{2\omega}{4\omega + 4}. \quad (5.20)$$

Let us then define

$$N_{\text{min}}(k, \omega) = \begin{cases} \frac{k\omega^2 + 2}{4\omega + 4} + b, & \text{if } \omega \text{ is odd} \\ \frac{k\omega^2 + 2}{4\omega + 4} - \frac{2\omega}{4\omega + 4} + b, & \text{if } \omega \text{ is even} \end{cases} \quad (5.21)$$

where $0 \leq b < 1$ is a bookkeeping device that rounds to the closest upper integer if ω is odd, or to the closest upper half-integer if ω is even, as required by the GSO-projection of eq. (5.7). Note that there is no upper bound on the levels, on the other hand. Furthermore, $N_{\text{min}}(k, \omega)$ is an increasing function of both k and, more importantly, ω . This means that the lowest allowed levels appear for $\omega = 1$.

As for the spectrally flowed continuous representations (that are analysed in Section 5.1), the lowest energy states are those for which either N_{tot} or \bar{N}_{tot} (or both) attain their lowest possible values. Let us first fix $\bar{N}_{\text{tot}} = N_{\text{min}}(k, \omega)$. Then by level-matching the spin s is positive or null. Furthermore, we fix $\bar{r} = -N_{\text{min}}(k, \omega) - 1/2$ if ω is even, and $\bar{r} = -N_{\text{min}}(k, \omega)$ if ω is odd. (Note that this is only possible if $N' = N'' = 0$, namely the internal CFT is not excited; this condition will lead to the analog of the even spin lowest energy states in the unflowed case.) This uniquely determines j to be

$$j = \frac{1}{2} \left(1 - k\omega + \sqrt{4bk(\omega + 1) + (k\omega - 1)^2} \right) \quad (5.22)$$

for both even and odd ω . We see that when $b = 0$ we indeed get $j = 0$, as expected. The energy is then given by

$$\begin{aligned} E_{\text{disc}}(s) &= s + \frac{k\omega}{2} + \frac{1}{\omega} \left(-\frac{2j(j-1)}{k} + 2N_{\text{min}}(k, \omega) - 1 \right) \\ &= s + \sqrt{4bk(\omega + 1) + (k\omega - 1)^2} - 2b - \frac{\omega(k\omega - 2)}{2(\omega + 1)} \end{aligned} \quad (5.23)$$

for odd ω , with a similar expression for even ω . As for the continuous case, for any even $\omega \geq 2$, the discrete $(\omega - 1)$ -sector has lower energy. Hence we restrict our attention to the case of odd ω , with energy given by (5.23). We find that the lowest energy states of positive

helicity s are then given by

$$\begin{aligned}
\omega \text{ even:} \quad N_{\text{tot}} &= N_{\text{min}}(k, \omega) + \omega s & m &= j - N_{\text{min}}(k, \omega) - \frac{1}{2} + s \\
&\bar{N}_{\text{tot}} = N_{\text{min}}(k, \omega) & \bar{m} &= j - N_{\text{min}}(k, \omega) - \frac{1}{2} \\
\omega \text{ odd:} \quad N_{\text{tot}} &= N_{\text{min}}(k, \omega) + \omega s & m &= j - N_{\text{min}}(k, \omega) + s \\
&\bar{N}_{\text{tot}} = N_{\text{min}}(k, \omega) & \bar{m} &= j - N_{\text{min}}(k, \omega).
\end{aligned} \tag{5.24}$$

We should note that the left-moving states do not saturate the value of m for the given value of N_{tot} , and thus they may have multiplicities greater than one. The right-moving states, on the other hand, saturate them, and hence will be unique. Finally, in the above we have assumed $s > 0$; the corresponding lightest states with negative helicity are obtained upon exchanging the roles of left- and right-movers.

Even though it is perhaps not evident, the leading energy (5.23) is an increasing function of ω , a fact which we have confirmed numerically. Therefore, the lowest energy states for any given spin come from the $\omega = 1$ sector. Their energy is

$$E_{\text{disc}}(s) = |s| + \sqrt{8bk + (k-1)^2} - 2b - \frac{k}{4} + \frac{1}{2}. \tag{5.25}$$

We emphasize that the parameter b introduced above is uniquely fixed by k and does not depend on the spin s . As a result, this dispersion relation is linear in the spin s . The same is also true for the states from the spectrally flowed continuous representations, see eq. (5.13). This behaviour ties in nicely with the observation of [51], see also [52], about the behaviour of classical strings for large spin s . In particular, it is argued in [51], see eq. (6.0.8), that the $\log s$ term correction term to the linear dispersion relation vanishes for pure NS-NS flux.¹⁵

5.3 Comparison of the different sectors

We can now compare the different dispersion relations coming from the different sectors. Recall from the analysis of Section 4.2, see eq. (4.7), that the dispersion relation for the leading Regge trajectory states from the unflowed discrete representations is

$$E_{\text{Regge}}(s) = 1 + \sqrt{1 + 2k(s-2)}, \tag{5.26}$$

where we have set $s = 2n + 2$ in eq. (4.7) — this corresponds to the top component of the corresponding $\mathcal{N} = 4$ multiplet — and expressed n in terms of s . These states are only available for spins up $s < \frac{k}{2} + 2 - \frac{1}{2k}$, see eq. (5.1). (Note that, for $k \geq 2$, the right-hand-side of this inequality is not an integer and hence cannot be attained.¹⁶) It is easy to see that (in

¹⁵These claims are somewhat in tension with the analysis of [53] where a $(\log s)^2$ correction term was found for the case of pure NS-NS flux. Our findings seem to support the conclusion of [51, 52]. We thank Arkady Tseytlin for drawing our attention to the work of [51].

¹⁶For $k = 1$, it gives $s = \pm 2$.

this range of spins) $E_{\text{Regge}}(s)$ from eq. (5.26) is smaller than both $E_{\text{cont}}(s)$ from eq. (5.13) or $E_{\text{disc}}(s)$ from eq. (5.25); in fact, precisely at the (unphysical) value $s = \frac{k}{2} + 2 - \frac{1}{2k}$ we have

$$E_{\text{Regge}}\left(s = \frac{k}{2} + 2 - \frac{1}{2k}\right) = 1 + k = E_{\text{cont}}\left(s = \frac{k}{2} + 2 - \frac{1}{2k}\right). \quad (5.27)$$

Thus the states from the unflowed discrete representations describe the leading Regge states for spins $s < \frac{k}{2} + 2 - \frac{1}{2k}$.

For larger spins, on the other hand, the relevant states must come from the spectrally flowed representations. As we have seen in sections 5.1 and 5.2, for both the spectrally flowed continuous and discrete representations, the lowest energy states always appear for $\omega = 1$, and in either case, they give rise to states of arbitrarily high spin. We can compare the relevant dispersion relations, and it is fairly straightforward to see from eqs. (5.13) and (5.25) that

$$E_{\text{cont}}(s) < E_{\text{disc}}(s) \quad (5.28)$$

for all spins. Thus it follows that the remaining states of the leading Regge trajectory are part of the spectrally flowed continuous representations. In order to get a sense of the qualitative picture, we have plotted the relevant states in Figure 1 for one representative value of k ($k = 20$).

The picture that emerges is thus that the lowest energy states arise in the unflowed discrete sector for as high spin as allowed by the MO-bound. Once the MO-bound is reached, the continuous $\omega = 1$ representations take over; this makes intuitive sense since the leading Regge trajectory states come from highly spinning strings that get longer and longer as the spin is increased. As they hit the boundary of AdS_3 , they merge into the continuum of long strings [16], and thus the leading Regge trajectory states of higher spin will arise from that part of the spectrum, i.e., from the spectrally flowed continuous representations.

6 Conclusions

In this paper we have studied string theory on the background $\text{AdS}_3 \times \text{S}^3 \times \text{T}^4$ with pure NS-NS flux, using the WZW model worldsheet description with a view to exhibiting the emergence of a higher spin symmetry in the tensionless (small level) limit. As we have shown in Section 3, this part of the moduli space does not contain a conventional tensionless point where small string excitations become massless and give rise to a Vasiliev higher spin theory. However, for $k = 1$, a stringy massless higher spin spectrum emerges from the spectrally flowed continuous representations (corresponding to long strings). These higher spin fields are of a different nature than those arising in the symmetric orbifold of T^4 [26], but they realise nicely some of the predictions of [23].

For generic values of k we could also identify quite convincingly the states that make up the leading Regge trajectory, and we saw that they comprise the spectrum of a Vasiliev higher spin theory with $\mathcal{N} = 4$ superconformal symmetry. It would be very interesting to try to repeat the above analysis using the worldsheet description of [28] that allows for the

description of the theory with pure R-R flux (where one would expect the actual higher spin symmetry to emerge, see the arguments of the Introduction). Among other things one should expect that the massless higher spin fields that arise from the long string spectrum at $k = 1$ will acquire a mass since the long string spectrum is believed to be a specific feature of the pure NS-NS background. On the other hand, the leading Regge trajectory states should become massless as one flows to the theory with pure R-R flux. It would be very interesting to confirm these expectations. It would also be very interesting to analyse to which extent the leading Regge trajectory forms a closed subsector of string theory in the tensionless limit.

Acknowledgments

It is a pleasure to thank Marco Baggio, Shouvik Datta, Jan de Boer, Lorenz Eberhardt, Diego Hofman, Chris Hull, Wei Li, Charlotte Sleight, Massimo Taronna, and in particular Rajesh Gopakumar, for useful discussions. MRG thanks the Galileo Galilei Institute for Theoretical Physics (GGI) for the hospitality and INFN for partial support during the completion of this work, within the program “New Developments in AdS3/CFT2 Holography”. JIJ thanks the University of Amsterdam String Theory Group, and the Nordic Institute for Theoretical Physics (NORDITA) within the program “Black Holes and Emergent Spacetime”, for their kind hospitality during the course of this work. This research was also (partly) supported by the NCCR SwissMAP, funded by the Swiss National Science Foundation.

A Supersymmetric current algebras: conventions and useful formulae

The $\mathcal{N} = 1$ superconformal WZW model is generated by a bosonic Kac-Moody algebra \mathfrak{g} , coupled to fermions in the adjoint representation

$$J^a(z)J^b(w) \sim \frac{if^ab_c J^c(w)}{z-w} + \frac{k\eta^{ab}}{(z-w)^2} \quad (\text{A.1})$$

$$J^a(z)\psi^b(w) \sim \frac{if^ab_c \psi^c(w)}{z-w} \quad (\text{A.2})$$

$$\psi^a(z)\psi^b(w) \sim \frac{k\eta^{ab}}{z-w} . \quad (\text{A.3})$$

In terms of modes,

$$[J_m^a, J_n^b] = if^ab_c J_{m+n}^c + km\eta^{ab}\delta_{m,-n} \quad (\text{A.4})$$

$$[J_m^a, \psi_r^b] = if^ab_c \psi_{m+r}^c \quad (\text{A.5})$$

$$\{\psi_r^a, \psi_s^b\} = k\eta^{ab}\delta_{r,-s} . \quad (\text{A.6})$$

The structure constants satisfy $f_c^{ab} = -f_c^{ba}$ by definition; moreover, f^{abc} can be chosen to be completely anti-symmetric (for a semi-simple Lie algebra). In addition, the Jacobi identity reads

$$f_d^{ab} f_e^{dc} + f_d^{ca} f_e^{db} + f_d^{bc} f_e^{da} = 0, \quad (\text{A.7})$$

and the dual Coxeter number h^\vee may be defined through

$$f_{bc}^d f^{abc} = 2h^\vee \eta^{ad}. \quad (\text{A.8})$$

We can decouple the fermions from the bosons by defining the shifted currents \mathcal{J}^a as

$$\mathcal{J}^a = J^a + \frac{i}{2k} f_{bc}^a (\psi^b \psi^c), \quad (\text{A.9})$$

where the round brackets denote normal ordering. Because of the anti-symmetry of the structure constants, this is trivial in the NS-sector, but there is a subtle contribution in the R-sector since we have — we follow the conventions of [54], see in particular eq. (3.1.43),

$$(\psi^a \psi^b)_p = \frac{1}{2} [\psi_0^a, \psi_p^b] + \sum_{m \leq -1} \psi_m^a \psi_{p-m}^b - \sum_{m \geq 1} \psi_{p-m}^b \psi_m^a. \quad (\text{A.10})$$

With this definition, the OPEs become

$$\mathcal{J}^a(z) \mathcal{J}^b(w) \sim \frac{i f_c^{ab} \mathcal{J}^c(w)}{z-w} + \frac{\kappa \eta^{ab}}{(z-w)^2} \quad (\text{A.11})$$

$$\mathcal{J}^a(z) \psi^b(w) \sim 0, \quad (\text{A.12})$$

where $\kappa \equiv k - h^\vee$, and h^\vee is the dual Coxeter number defined in (A.8). Equivalently, in terms of modes we find

$$[\mathcal{J}_m^a, \mathcal{J}_n^b] = i f_c^{ab} \mathcal{J}_{m+n}^c + \kappa m \eta^{ab} \delta_{m,-n} \quad (\text{A.13})$$

$$[\mathcal{J}_m^a, \psi_r^b] = 0. \quad (\text{A.14})$$

Hence, the algebra is isomorphic to the direct (commuting) sum of a bosonic affine algebra at shifted level κ , and $\dim(\mathfrak{g})$ free fermions.

Using the above shifted currents we obtain the stress tensor and a dimension-3/2 supercurrent via the Sugawara construction,

$$T = \frac{1}{2k} \eta_{ab} \left[(\mathcal{J}^a \mathcal{J}^b) - (\psi^a \partial \psi^b) \right] \quad (\text{A.15})$$

$$G = \frac{1}{k} \left[\eta_{ab} \mathcal{J}^a \psi^b - \frac{i f_{abc}}{6k} (\psi^a \psi^b \psi^c) \right], \quad (\text{A.16})$$

where the round brackets denote normal-ordering, and the triple product is defined recursively, i.e., $(\psi^a \psi^b \psi^c) \equiv (\psi^a (\psi^b \psi^c))$.¹⁷ These fields satisfy the $\mathcal{N} = 1$ superconformal

¹⁷Because of the total anti-symmetry of the structure constants, normal ordering is again trivial in the NS-sector, but there is a contribution coming from the commutator term in (A.10).

algebra

$$T(z)T(w) \sim \frac{c/2}{(z-w)^4} + \frac{2T(w)}{(z-w)^2} + \frac{\partial T(w)}{z-w} \quad (\text{A.17})$$

$$T(z)G(w) \sim \frac{3}{2} \frac{G(w)}{(z-w)^2} + \frac{\partial G(w)}{z-w} \quad (\text{A.18})$$

$$G(z)G(w) \sim \frac{2c/3}{(z-w)^3} + \frac{2T(w)}{z-w} \quad (\text{A.19})$$

with central charge

$$c = \dim(\mathfrak{g}) \left(\frac{k - h^\vee}{k} + \frac{1}{2} \right) = \dim(\mathfrak{g}) \left(\frac{\kappa}{\kappa + h^\vee} + \frac{1}{2} \right). \quad (\text{A.20})$$

In terms of modes, in the NS sector we have

$$[L_m, L_n] = (m-n)L_{m+n} + \frac{c}{12} m(m^2-1) \delta_{m,-n} \quad (\text{A.21})$$

$$[L_n, G_r] = \left(\frac{n}{2} - r \right) G_{n+r} \quad (\text{A.22})$$

$$\{G_r, G_s\} = 2L_{r+s} + \frac{c}{3} \left(r^2 - \frac{1}{4} \right) \delta_{r,-s}. \quad (\text{A.23})$$

Due to the non-trivial R-sector normal ordering term, see eq. (A.10), for the above definition of the normal ordered modes we obtain in the R-sector the algebra

$$[L_m, L_n] = (m-n)L_{m+n} + m \frac{\dim(\mathfrak{g})}{8} \left(m^2 - \frac{2h^\vee}{3k} (m^2-1) \right) \delta_{m,-n} \quad (\text{A.24})$$

$$[L_n, G_r] = \left(\frac{n}{2} - r \right) G_{r+n} \quad (\text{A.25})$$

$$\{G_r, G_s\} = 2L_{r+s} + \frac{c}{3} s^2 \delta_{r,-s} + \frac{h^\vee \dim(\mathfrak{g})}{12k} \delta_{r,-s} \quad (\text{A.26})$$

instead. Note in particular that the Virasoro commutator $[L_m, L_n]$ does not have the standard form. If so desired, this can be rectified by shifting the zero mode of the stress tensor as

$$L_n \rightarrow L_n^R = L_n + \frac{\dim(\mathfrak{g})}{16} \delta_{n,0}, \quad (\text{A.27})$$

so that the superconformal algebra then reads

$$[L_m^R, L_n^R] = (m-n)L_{m+n}^R + \frac{c}{12} m(m^2-1) \delta_{m,-n} \quad (\text{A.28})$$

$$[L_n^R, G_r] = \left(\frac{n}{2} - r \right) G_{n+r} \quad (\text{A.29})$$

$$\{G_r, G_s\} = 2L_{r+s}^R + \frac{c}{3} \left(r^2 - \frac{1}{4} \right) \delta_{r,-s}, \quad (\text{A.30})$$

which is exactly as in the NS sector. The price one pays for this redefinition is that the fermionic Ramond vacuum $|0\rangle_R$ (which is annihilated by all the positive modes of the fermions) is no longer annihilated by L_0 , but rather satisfies

$$L_0^R |0\rangle_R = \frac{\dim(\mathfrak{g})}{16} |0\rangle_R \quad (\text{A.31})$$

instead.

Finally, it is interesting to note that if we simultaneously consider supersymmetric $\mathfrak{sl}(2, \mathbb{R})$ and $\mathfrak{su}(2)$ algebras (which have h^\vee equal and opposite in sign), as appropriate to $\text{AdS}_3 \times \text{S}^3$, we find that the h^\vee terms in (A.24) – (A.26) drop out from the algebra of the total currents.

B Low momenta subtleties

The only subtlety concerning the counting of physical states given by eqs. (4.1) and (4.2) arises for $j = 1$ and $j' = 0$. Then the mass-shell condition requires that the physical states appear at excitation number $N = \frac{1}{2}$, and in particular, the state that is excited by $\psi_{-1/2}^-$ has $j = 0$. For $j = 0$ the general character formula for $\mathfrak{sl}(2, \mathbb{R})$ representations (4.4) breaks down since the $L_{-1} = J_0^+$ descendant of the state with $j = 0$ is null. As a consequence, we have the identity

$$\frac{y^0}{1-y} = 1 + \frac{y}{1-y} = \chi_{j=0} + \chi_{j=1} , \quad (\text{B.1})$$

i.e., the character on the left-hand-side is actually not an irreducible character, but rather splits up into the contributions of two different irreducible $\mathfrak{sl}(2, \mathbb{R})$ representations (namely the ones with $j = 0$ and $j = 1$). This phenomenon also has a microscopic origin: for $j = 1$ and $j' = 0$ there are three $\mathfrak{sl}(2, \mathbb{R})$ descendants that define physical states, namely

$$|\frac{1}{2}; 2, 2\rangle = \psi_{-1/2}^- |1, 3\rangle - 6\psi_{-1/2}^3 |1, 2\rangle + 6\psi_{-1/2}^+ |1, 1\rangle \quad (\text{B.2})$$

$$|\frac{1}{2}; 1, 1\rangle = \psi_{-1/2}^- |1, 2\rangle - 2\psi_{-1/2}^3 |1, 1\rangle \quad (\text{B.3})$$

$$|\frac{1}{2}; 0, 0\rangle = \psi_{-1/2}^- |1, 1\rangle , \quad (\text{B.4})$$

and one easily confirms that all three of them are physical. (And, in fact, $|\frac{1}{2}; 1, 1\rangle = J_0^+ |\frac{1}{2}; 0, 0\rangle$, reflecting the null-vector structure mentioned before.)

Since one of these states ($|\frac{1}{2}; 0, 0\rangle$) is the vacuum state of the space-time CFT, these states describe the chiral states of the space-time CFT. (Recall that the above discussion is a chiral discussion; the vacuum state for the right-movers, say, appears then together with the above states.) In particular, the $j = h = 2$ state is the Virasoro field, and at $j = h = 1$ we get in addition to the state $|\frac{1}{2}; 1, 1\rangle$ six $j = h = 1$ states from the excitations associated to the $\text{S}^3 \times \text{T}^4$ directions. Altogether, they give rise to an $\mathfrak{su}(2)$ current algebra (coming from the S^3 excitations), as well as four $h = 1$ bosons — these are the familiar bosons of the T^4 . (Similarly, in the R-sector we get four $h = \frac{1}{2}$ fields and four $h = \frac{3}{2}$ fields — they describe the four free fermions of the T^4 , as well as the four supercharges of the $\mathcal{N} = 4$ superconformal algebra.)

C The structure of small $\mathcal{N} = 4$ multiplets

The (small) $\mathcal{N} = 4$ superconformal algebra is generated by a Virasoro algebra with modes L_n , an affine $\mathfrak{su}(2)$ algebra with modes T_n^a (where $a = \pm, 3$), as well as four supercharges $Q^{i\pm}$ where $i = 1, 2$. (The supercharges transform as two doublets with respect to the $\mathfrak{su}(2)$ algebra). The commutation relations are of the form

$$\begin{aligned}
[L_m, L_n] &= (m-n)L_{m+n} + \frac{c}{12}m(m^2-1)\delta_{m+n,0} \\
[L_m, T_n^a] &= -nT_{m+n}^a \\
[L_m, Q_n^{i\pm}] &= \left(\frac{m}{2} - n\right) Q_{m+n}^{i\pm} \\
[T_m^3, T_n^\pm] &= \pm T_{m+n}^\pm \\
[T_m^3, T_n^3] &= \frac{c}{12}m\delta_{m+n,0} \\
[T_m^+, T_n^-] &= 2T_{m+n}^3 + \frac{c}{6}m\delta_{m+n,0} \\
[T_m^3, Q_n^{i\pm}] &= \pm \frac{1}{2}Q_{m+n}^{i\pm}, \quad [T_m^\pm, Q_n^{i\pm}] = 0 \\
[T_m^\pm, Q_n^{1\mp}] &= -Q_{m+n}^{1\pm}, \quad [T_m^\pm, Q_n^{2\mp}] = Q_{m+n}^{2\pm} \\
\{Q_m^{i\pm}, Q_n^{i\pm}\} &= \{Q_m^{i\pm}, Q_n^{i\mp}\} = 0 \\
\{Q_m^{1\pm}, Q_n^{2\mp}\} &= 2L_{m+n} \pm 2(m-n)T_{m+n}^3 + \frac{c}{3}(m^2 - \frac{1}{4})\delta_{m+n,0} \\
\{Q_m^{1\pm}, Q_n^{2\pm}\} &= -2(m-n)T_{m+n}^\pm
\end{aligned} \tag{C.1}$$

where the central charge is $c = 6k$. We denote the corresponding right-moving generators as \bar{L}_n , $\bar{Q}^{i\pm}$, and \bar{T}_n^a .

With these preparations we can now describe the structure of the supermultiplets. We shall first concentrate on the chiral (say left-moving) algebra and describe the representations of the (small) $\mathcal{N} = 4$ superconformal algebra, keeping track of the $\mathfrak{su}(2)$ quantum numbers. Following the notation in [44], we will label $\mathfrak{su}(2)$ representations by their dimension $m = 2j' + 1$. A generic multiplet has then the form, see Table 6.

state	$\mathfrak{su}(2)$	h
$ m\rangle$	\mathbf{m}	h
$Q m\rangle$	$2 \cdot (\mathbf{m} + \mathbf{1}) \oplus 2 \cdot (\mathbf{m} - \mathbf{1})$	$h + 1/2$
$QQ m\rangle$	$4 \cdot \mathbf{m} \oplus (\mathbf{m} + \mathbf{2}) \oplus (\mathbf{m} - \mathbf{2})$	$h + 1$
$QQQ m\rangle$	$2 \cdot (\mathbf{m} + \mathbf{1}) \oplus 2 \cdot (\mathbf{m} - \mathbf{1})$	$h + 3/2$
$QQQQ m\rangle$	\mathbf{m}	$h + 2$

Table 6. Chiral long $\mathcal{N} = 4$ multiplet.

For small values of \mathbf{m} , namely $\mathbf{m} = 1$ and $\mathbf{m} = 2$, there are various shortenings; more specifically, we find for $\mathbf{m} = 1$ and $\mathbf{m} = 2$ the shorter multiplets, see Table 7.

If we denote the highest weight state as $|h; j'\rangle$, the $\frac{1}{4}$ BPS bound for the above algebra

state	$\mathfrak{su}(2)$	h	state	$\mathfrak{su}(2)$	h
$ 1\rangle$	$\mathbf{1}$	h	$ 2\rangle$	$\mathbf{2}$	h
$Q 1\rangle$	$2 \cdot \mathbf{2}$	$h + 1/2$	$Q 2\rangle$	$2 \cdot \mathbf{3} \oplus 2 \cdot \mathbf{1}$	$h + 1/2$
$QQ 1\rangle$	$\mathbf{3} \oplus 3 \cdot \mathbf{1}$	$h + 1$	$QQ 2\rangle$	$\mathbf{4} \oplus 4 \cdot \mathbf{2}$	$h + 1$
$QQQ 1\rangle$	$2 \cdot \mathbf{2}$	$h + 3/2$	$QQQ 2\rangle$	$2 \cdot \mathbf{3} \oplus 2 \cdot \mathbf{1}$	$h + 3/2$
$QQQQ 1\rangle$	$\mathbf{1}$	$h + 2$	$QQQQ 2\rangle$	$\mathbf{1}$	$h + 2$

Table 7. Chiral long $\mathcal{N} = 4$ multiplet for $\mathbf{m} = 1$ and $\mathbf{m} = 2$.

is obtained by demanding that $Q_{-1/2}^{i+} |h; j'\rangle = 0$ for one choice of $i \in \{1, 2\}$. Using that

$$\left\{ Q_{1/2}^{2-}, Q_{-1/2}^{1+} \right\} = \left\{ Q_{1/2}^{1-}, Q_{-1/2}^{2+} \right\} = 2(L_0 - T_0^3) , \quad (\text{C.2})$$

we see that every $\frac{1}{4}$ BPS state is automatically $\frac{1}{2}$ BPS, i.e., if $Q_{-1/2}^{i+} |h; j'\rangle = 0$ for one choice of i , it is actually zero for both $i = 1, 2$. Furthermore, the BPS bound is explicitly

$$\text{BPS bound:} \quad (L_0 - T_0^3) |h; j'\rangle = 0 \quad \implies \quad h = j' . \quad (\text{C.3})$$

The resulting short multiplet is described in table 8. As usual, for small values of j' (or \mathbf{m}), there are further shortenings, in particular, for $\mathbf{m} = 1$ the whole multiplet consists just of the vacuum itself $h = j' = 0$, while for $\mathbf{m} = 2$ the whole multiplet truncates to $\mathbf{2} (h = \frac{1}{2}) \oplus 2 \cdot \mathbf{1} (h = 1)$.

state	$\mathfrak{su}(2)$	h
$ m\rangle$	\mathbf{m}	j'
$Q m\rangle$	$2 \cdot (\mathbf{m} - \mathbf{1})$	$j' + 1/2$
$QQ m\rangle$	$\mathbf{m} - \mathbf{2}$	$j' + 1$

Table 8. Chiral BPS multiplet. (Recall that $m = 2j' + 1$.)

The corresponding multiplets of the full $(4, 4)$ theory is then obtained by tensoring these chiral multiplets together. For example, if both left- and right-moving multiplets are long (corresponding to \mathbf{m} and $\bar{\mathbf{m}}$), the total number of states is $256 \times m \cdot \bar{m}$.

References

- [1] D. J. Gross, *High-Energy Symmetries of String Theory*, *Phys. Rev. Lett.* **60** (1988) 1229.
- [2] E. Witten, *Space-time and Topological Orbifolds*, *Phys. Rev. Lett.* **61** (1988) 670.
- [3] G. W. Moore, *Symmetries and symmetry breaking in string theory*, in *International Workshop on Supersymmetry and Unification of Fundamental Interactions (SUSY 93) Boston, Massachusetts, March 29-April 1, 1993*, pp. 0540–552, 1993. [hep-th/9308052](#).
- [4] B. Sundborg, *Stringy gravity, interacting tensionless strings and massless higher spins*, *Nucl.Phys.Proc.Suppl.* **102** (2001) 113–119, [[hep-th/0103247](#)].
- [5] A. Mikhailov, *Notes on higher spin symmetries*, [hep-th/0201019](#).

- [6] M. A. Vasiliev, *Nonlinear equations for symmetric massless higher spin fields in (A)dS(d)*, *Phys. Lett.* **B567** (2003) 139–151, [[hep-th/0304049](#)].
- [7] M. R. Gaberdiel and R. Gopakumar, *Higher Spins & Strings*, *JHEP* **11** (2014) 044, [[1406.6103](#)].
- [8] J. R. David, G. Mandal and S. R. Wadia, *Microscopic formulation of black holes in string theory*, *Phys. Rept.* **369** (2002) 549–686, [[hep-th/0203048](#)].
- [9] M. R. Gaberdiel and R. Gopakumar, *Large $\mathcal{N} = 4$ Holography*, *JHEP* **1309** (2013) 036, [[1305.4181](#)].
- [10] S. F. Prokushkin and M. A. Vasiliev, *Higher spin gauge interactions for massive matter fields in 3-D AdS space-time*, *Nucl.Phys.* **B545** (1999) 385, [[hep-th/9806236](#)].
- [11] S. F. Prokushkin and M. A. Vasiliev, *3-d higher spin gauge theories with matter*, [[hep-th/9812242](#)].
- [12] M. R. Gaberdiel and R. Gopakumar, *An AdS₃ Dual for Minimal Model CFTs*, *Phys.Rev.* **D83** (2011) 066007, [[1011.2986](#)].
- [13] M. R. Gaberdiel and R. Gopakumar, *Minimal Model Holography*, *J.Phys.* **A46** (2013) 214002, [[1207.6697](#)].
- [14] M. Beccaria, C. Candu and M. R. Gaberdiel, *The large $N = 4$ superconformal W_∞ algebra*, *JHEP* **06** (2014) 117, [[1404.1694](#)].
- [15] M. R. Gaberdiel and C. Peng, *The symmetry of large $\mathcal{N} = 4$ holography*, *JHEP* **05** (2014) 152, [[1403.2396](#)].
- [16] J. M. Maldacena and H. Ooguri, *Strings in AdS₃ and the SL(2, \mathbb{R}) WZW model. The Spectrum*, *J. Math. Phys.* **42** (2001) 2929–2960, [[hep-th/0001053](#)].
- [17] J. M. Maldacena, H. Ooguri and J. Son, *Strings in AdS₃ and the SL(2, \mathbb{R}) WZW model. Euclidean black hole*, *J. Math. Phys.* **42** (2001) 2961–2977, [[hep-th/0005183](#)].
- [18] J. M. Maldacena and H. Ooguri, *Strings in AdS₃ and the SL(2, \mathbb{R}) WZW model. Part 3. Correlation functions*, *Phys. Rev.* **D65** (2002) 106006, [[hep-th/0111180](#)].
- [19] J. Isberg, U. Lindstrom, B. Sundborg and G. Theodoridis, *Classical and quantized tensionless strings*, *Nucl. Phys.* **B411** (1994) 122–156, [[hep-th/9307108](#)].
- [20] A. Sagnotti and M. Tsulaia, *On higher spins and the tensionless limit of string theory*, *Nucl. Phys.* **B682** (2004) 83–116, [[hep-th/0311257](#)].
- [21] A. Bagchi, S. Chakraborty and P. Parekh, *Tensionless Superstrings: View from the Worldsheet*, *JHEP* **10** (2016) 113, [[1606.09628](#)].
- [22] A. Bagchi, S. Chakraborty and P. Parekh, *Tensionless Strings from Worldsheet Symmetries*, *JHEP* **01** (2016) 158, [[1507.04361](#)].
- [23] N. Seiberg and E. Witten, *The D1 / D5 system and singular CFT*, *JHEP* **04** (1999) 017, [[hep-th/9903224](#)].
- [24] S. Elitzur, O. Feinerman, A. Giveon and D. Tsabar, *String theory on AdS₃ × S³ × S³ × S¹*, *Phys. Lett.* **B449** (1999) 180–186, [[hep-th/9811245](#)].
- [25] L. Eberhardt, M. R. Gaberdiel, R. Gopakumar and W. Li, *BPS spectrum on AdS₃ × S³ × S³ × S¹*, *JHEP* **03** (2017) 124, [[1701.03552](#)].
- [26] M. R. Gaberdiel, R. Gopakumar and C. Hull, *Stringy AdS₃ from the Worldsheet*, to appear.

- [27] K. Ferreira, *Even spin $\mathcal{N} = 4$ holography*, [1702.02641](#).
- [28] N. Berkovits, C. Vafa and E. Witten, *Conformal field theory of AdS background with Ramond-Ramond flux*, *JHEP* **03** (1999) 018, [[hep-th/9902098](#)].
- [29] A. Giveon, D. Kutasov and N. Seiberg, *Comments on string theory on AdS₃*, *Adv. Theor. Math. Phys.* **2** (1998) 733–780, [[hep-th/9806194](#)].
- [30] A. Pakman, *Unitarity of supersymmetric $SL(2,R) / U(1)$ and no ghost theorem for fermionic strings in $AdS(3) \times N$* , *JHEP* **01** (2003) 077, [[hep-th/0301110](#)].
- [31] D. Israel, C. Kounnas and M. P. Petropoulos, *Superstrings on NS5 backgrounds, deformed $AdS(3)$ and holography*, *JHEP* **10** (2003) 028, [[hep-th/0306053](#)].
- [32] S. Raju, *Counting giant gravitons in $AdS(3)$* , *Phys. Rev.* **D77** (2008) 046012, [[0709.1171](#)].
- [33] I. T. Ivanov, B.-b. Kim and M. Rocek, *Complex structures, duality and WZW models in extended superspace*, *Phys. Lett.* **B343** (1995) 133–143, [[hep-th/9406063](#)].
- [34] S. Gerigk, *Superstring theory on $AdS_3 \times S^3$ and the $PSL(2|2)$ WZW model*. PhD thesis, ETH Zürich, 2012.
- [35] S. Hwang, *No ghost theorem for $SU(1,1)$ string theories*, *Nucl. Phys.* **B354** (1991) 100–112.
- [36] J. M. Evans, M. R. Gaberdiel and M. J. Perry, *The no ghost theorem for AdS₃ and the stringy exclusion principle*, *Nucl. Phys.* **B535** (1998) 152–170, [[hep-th/9806024](#)].
- [37] U. Lindstrom and M. Zabzine, *Tensionless strings, WZW models at critical level and massless higher spin fields*, *Phys. Lett.* **B584** (2004) 178–185, [[hep-th/0305098](#)].
- [38] I. Bakas and C. Sourdis, *On the tensionless limit of gauged WZW models*, *JHEP* **06** (2004) 049, [[hep-th/0403165](#)].
- [39] M. Bershadsky, S. Zhukov and A. Vaintrob, *$PSL(n/n)$ sigma model as a conformal field theory*, *Nucl. Phys.* **B559** (1999) 205–234, [[hep-th/9902180](#)].
- [40] G. Gotz, T. Quella and V. Schomerus, *The WZNW model on $PSU(1,1|2)$* , *JHEP* **03** (2007) 003, [[hep-th/0610070](#)].
- [41] J. Balog, L. O’Raifeartaigh, P. Forgacs and A. Wipf, *Consistency of String Propagation on Curved Space-Times: An $SU(1,1)$ Based Counterexample*, *Nucl. Phys.* **B325** (1989) 225.
- [42] P. M. S. Petropoulos, *Comments on $SU(1,1)$ string theory*, *Phys. Lett.* **B236** (1990) 151–158.
- [43] L. J. Dixon, M. E. Peskin and J. D. Lykken, *$N=2$ Superconformal Symmetry and $SO(2,1)$ Current Algebra*, *Nucl. Phys.* **B325** (1989) 329–355.
- [44] J. de Boer, *Six-dimensional supergravity on $S^3 \times AdS_3$ and 2-D conformal field theory*, *Nucl.Phys.* **B548** (1999) 139–166, [[hep-th/9806104](#)].
- [45] O. Aharony, S. S. Gubser, J. M. Maldacena, H. Ooguri and Y. Oz, *Large N field theories, string theory and gravity*, *Phys. Rept.* **323** (2000) 183–386, [[hep-th/9905111](#)].
- [46] M. R. Gaberdiel, C. Peng and I. G. Zadeh, *Higgsing the stringy higher spin symmetry*, *JHEP* **10** (2015) 101, [[1506.02045](#)].
- [47] R. Argurio, A. Giveon and A. Shomer, *Superstrings on $AdS(3)$ and symmetric products*, *JHEP* **12** (2000) 003, [[hep-th/0009242](#)].
- [48] G. Giribet, A. Pakman and L. Rastelli, *Spectral Flow in $AdS(3)/CFT(2)$* , *JHEP* **06** (2008) 013, [[0712.3046](#)].

- [49] M. R. Gaberdiel and R. Gopakumar, *String Theory as a Higher Spin Theory*, [1512.07237](#).
- [50] M. R. Gaberdiel and R. Gopakumar, *Stringy Symmetries and the Higher Spin Square*, *J. Phys.* **A48** (2015) 185402, [[1501.07236](#)].
- [51] A. Stepanchuk, *Aspects of integrability in string sigma-models*. PhD thesis, Imperial Coll., London, 2015.
- [52] A. Banerjee and A. Sadhukhan, *Multi-spike strings in AdS_3 with mixed three-form fluxes*, *JHEP* **05** (2016) 083, [[1512.01816](#)].
- [53] J. R. David and A. Sadhukhan, *Spinning strings and minimal surfaces in AdS_3 with mixed 3-form fluxes*, *JHEP* **10** (2014) 49, [[1405.2687](#)].
- [54] J. Fuchs, *Affine Lie algebras and quantum groups: An Introduction, with applications in conformal field theory*. Cambridge University Press, 1995.